Zebrafish *hif-3α* modulates erythropoiesis via regulation of *gata-1* to facilitate hypoxia tolerance

Xiaolian Cai[1,4], Ziwen Zhou[1,4], Junji Zhu[1,4], Qian Liao[1,4], Dawei Zhang[1], Xing Liu[1, 2, 5], Jing Wang[1, 2, 5], Gang Ouyang[1, 2, 5], Wuhan Xiao[1, 2, 3, 4, 5, *]

[1] State Key Laboratory of Freshwater Ecology and Biotechnology, Institute of Hydrobiology, Chinese Academy of Sciences; [2] The Key laboratory of Aquaculture Disease Control, Ministry of Agriculture; [3] The Key Laboratory of Aquatic Biodiversity and Conservation, Institute of Hydrobiology, Chinese Academy of Sciences, Wuhan, 430072, China; [4] University of Chinese Academy of Sciences, Beijing, 100049, China; [5] The Innovation of Seed Design, Chinese Academy of Sciences, Wuhan, 430072, China.

***Corresponding author**: Wuhan Xiao. Ph.D. Institute of Hydrobiology, Chinese Academy of Sciences, Wuhan, 430072, P.R. China

Phone: 86-27-68780087; Fax: 86-27-68780087; E-mail: w-xiao@ihb.ac.cn

KEY WORDS: *hif-3α*, *gata-1*, zebrafish, hypoxia, erythropoiesis

SUMMARY STATEMENT

Hif-3*α* directly regulates *gata-1* expression to modulate erythropoiesis, which enhances zebrafish hypoxia tolerance.

ABSTRACT

The hypoxia-inducible factors 1α and 2α (HIF-1α and HIF-2α) are master regulators of the cellular response to O_2. In addition to HIF-1α and HIF-2α, HIF-3α is another identified member of the HIF-α gene family. Even though whether some HIF-3α isoforms have transcriptional activity or repressive activity is still under debate, it is evident that the full length of HIF-3α acts as a transcription factor. However, its function in hypoxia signaling is largely unknown. Here, we showed that loss of *hif-3α* in zebrafish reduced hypoxia tolerance. Further assays indicated that erythrocyte number was decreased because red blood cell maturation was impeded by *hif-3α* disruption. We found that *gata-1* expression was downregulated in *hif-3α*-null zebrafish, as were several hematopoietic marker genes, including *alas2, band3, hbae1, hbae3* and *hbbe1*. *hif-3α* recognized the hypoxia response element (HRE) located in the promoter of *gata*-1 and directly bound to the promoter to transactivate *gata-1* expression. Our results suggested that *hif-3α* facilities hypoxia tolerance by modulating erythropoiesis via *gata-1* regulation.

INTRODUCTION

O_2 is indispensable for the survival of aerobic organism (Aragones et al., 2009; Majmundar et al., 2010; Semenza, 2014). Organisms have evolved sophisticated cellular sensors that respond to O_2 gradients (Bigham and Lee, 2014; Prabhakar and Semenza, 2015; Prabhakar and Semenza, 2016). Hypoxia is condition characterized by low ambient O_2, hypoxia triggers acute and chronic organismal responses and induces the expression of numerous genes (Semenza, 2014) (Aragones et al., 2009; Greer et al., 2012; Prabhakar and Semenza, 2012; Semenza, 2012; Shen and Kaelin, 2013). HIF-1α and HIF-2α are regulators of the cellular response to O_2 (Majmundar et al., 2010; Semenza, 2012; Semenza, 2014). Under normoxia, PHD1, PHD2, and PHD3 use O_2 and 2-oxoglutarate as substrates for the hydroxylation of HIF-1α and HIF-2α. Hydroxylated HIF-1α and HIF-2α are bound VHL protein. VHL recruits a ubiquitin ligase complex that targets HIF-1α and HIF-2α for proteasomal degradation. Hypoxia inhibits PHD enzymatic activity, preventing the PHDs from hydroxylating HIF-1α and HIF-2α. This results in HIF-α protein stabilization and the induction of transcriptional activity (Bishop and Ratcliffe, 2015; Semenza, 2014).

HIF-3α is another HIF-α gene (Augstein et al., 2011) (Duan, 2016a; Ravenna et al., 2016). Different from HIF-1α and HIF-2α, HIF-3α comprises a TAD (transactivation domain), a leucine zipper domain (LZIP), and an LXXLL motif (Gu et al., 1998; Zhang et al., 2012b). Therefore, HIF-3α may be functionally distinguishable from HIF-1α and HIF-2α. Mammalian HIF-3α genes unitize different promoters, different

transcription initiation sites, and alternative splicing to transcribe a large number of mRNA variants (Duan, 2016a). Some of these short HIF-3α isoforms lack TADs (Hara et al., 2001), and others have weak or absent transcriptional activity (Gu et al., 1998; Pasanen et al., 2010). Moreover, the overexpression of some HIF-3α isoforms suppresses HIF-1α- and/or HIF-2α-induced reporter activity in cells (Maynard et al., 2003) (Makino et al., 2001; Makino et al., 2007; Yamashita et al., 2008). Thus, it has been widely accepted that HIF-3α acts as a negative regulator of HIF-1α and HIF-2α, even though, to date, only partial variants of mammalian HIF-3α transcripts have been investigated, mostly via overexpression in cell culture systems with artificial reporter constructs (Duan, 2016a; Ravenna et al., 2016). However, multiple lines of evidence support that the full length of HIF-3α acts as a transcription factor (Duan, 2016b; Heikkila et al., 2011; Zhang et al., 2014; Zhou et al., 2018) .

Interestingly, in zebrafish, only two isoforms of HIF-3α (*hif-3α/hif-3α1* and *hif-3α2*) have been identified (Zhang et al., 2016; Zhang et al., 2012b; Zhang et al., 2014) (Makino et al., 2001). Zebrafish *hif-3α* is a hypoxia-induced transcription factor that activates gene expression distinct from HIF-1α (Zhang et al., 2014), while *hif-3α2* is an oxygen-insensitive nuclear protein that inhibits canonical Wnt signaling by binding to β-catenin and destabilizing the nuclear β-catenin complex (Zhang et al., 2016).

To date, the roles of HIF-3α in hypoxia signaling, and the mechanisms underlying these roles, are almost entirely unclear. Here, we knocked out *hif-3a* in zebrafish and found that the resulting mutants exhibited increased sensitivity to hypoxia and reduced erythropoiesis. Our mechanistic studies indicated that *hif-3a* acted as a transcription factor and directly regulated *gata-1* expression.

RESULTS AND DISSUCITION

Loss of hif-3a in zebrafish reduced hypoxia tolerance

Zebrafish carry two isoforms of *hif-3a*: *hif-3a/hif-3a1* (herein referred to as *hif-3a*) and *hif-3a2* (Fig. S1A and S1B) (Zhang et al., 2016; Zhang et al., 2012b; Zhang et al., 2014). We designed two gRNAs to disrupt the expression of this gene (Fig. S1A). Two mutants in the *hif-3a* gene: *hif-3a*$^{ihb20180620/ihb20180620}$ (http://zfin.org/ZDB-ALT-180620-1) herein designated M1, and *hif-3a*$^{ihb20180621/ihb20180621}$ (http://zfin.org/ZDB-ALT-180620-2) herein designated M2 were screened (Fig. S1A-C). The mutant *hif-3a* encoded two truncated peptides (Fig. S1B). *Hif-3a* mRNA expression was largely downregulated in the two mutants as compared to the wildtype (WT; Fig. S1D). An anti-hif-3*a* antibody had been developed and confirmed to recognize zebrafish hif-3a protein specifically (Zhang et al., 2012a). By Western blot analysis,

hif-3a protein could not be detected in the mutant (Fig. S1E). Overall, *hif-3a* $^{-/-}$ zebrafish were identical to their WT siblings (*hif-3a*$^{+/+}$) under normal conditions. Of note, the predicted truncated peptide of M1 contains the bHLH domain and that of M2 contains bHLH-PAS-PAC-ODD domains. The bHLH domain is important for DNA binding and dimerization with HIF-1β. The PAS-A/B and PAC domains are also involved in HIF-1β for dimerization (Semenza, 2014). To determine whether M1 and/or M2 mutant proteins may act in a dominant-negative manner, we examined overexpression of the predicted truncated peptides of M1 and M2 on an HRE-luciferase reporter activity. As shown in Figure S2A, S2B and S2C, overexpression of the predicted truncated peptides of M1 and M2 had no effect on the transcriptional activity of *hif-1ab*, *hif-1ab* and *hif-3a* in EPC cells (Fig. S2A, S2B and S2C). In the following experiments, we primarily used mutant M1 (*hif-3a*$^{ihb20180620/ihb20180620}$) for phenotype analysis, and confirmed the observed M1 phenotypes in M2 (*hif-3a*$^{ihb20180621/ihb20180621}$) to exclude off-targeting effects.

Given that *hif-3a* was identified as an oxygen-dependent factor (Zhang et al., 2014), we aimed to determine whether disruption of *hif-3a* impacted zebrafish hypoxia tolerance (Cai et al., 2018). In this study, after exposing *hif-3a* $^{+/+}$ and *hif-3a* $^{-/-}$ larvae to 2% O_2 simultaneously for 12 hours (h), more *hif-3a*$^{-/-}$ larvae were dead than *hif-3a*$^{+/+}$ larvae (Fig. 1A and B). Under normoxia (21% O_2), no significant differences were detected between *hif-3a*$^{+/+}$ and *hif-3a*$^{-/-}$ larvae (Fig. 1A, D).

Subsequently, we measured the hypoxia tolerance of adult zebrafish (3 mpf). When *hif-3a*$^{+/+}$ and *hif-3a*$^{-/-}$ adults with similar body weights (0.32 $\pm$ 0.02 g) were subjected to hypoxia (5% O_2, adjusted prior to experimentation) simultaneously for 30 min, there were no obvious differences in behavior (Video S1). However, the duration of hypoxia increased, two *hif-3a*$^{-/-}$ zebrafish appeared dead or near dead, while three *hif-3a*$^{+/+}$zebrafish remained active (Video S2).

Furthermore, we tested another set of adults (6 mpf). *hif-3a*$^{+/+}$ and *hif-3a*$^{-/-}$ adults (6 mpf), with similar body weights (0.65 $\pm$ 0.02 g), were subjected to hypoxia (5% O_2, adjusted prior to experimentation). After 30 min, no significant difference in behaviors was observed between the *hif-3a*$^{+/+}$ and *hif-3a*$^{-/-}$ (Fig. 1C). However, *hif-3a*$^{-/-}$ began to die after 46 min of hypoxia. After 50 min of hypoxia, all *hif-3a* $^{-/-}$ zebrafish were dead, and all *hif-3a*$^{+/+}$ zebrafish were still alive (Fig. 1C). Therefore, *hif-3a* $^{-/-}$ zebrafish were more sensitive to hypoxia compared with all *hif-3a*$^{+/+}$ zebrafish.

To determine whether the difference of hypoxia tolerance exhibited between *hif-3a*$^{+/+}$ and *hif-3a* $^{-/-}$ zebrafish was resulted from *hif-3a* $^{-/-}$ zebrafish having higher oxygen consumption. Unexpectedly, in fact, the oxygen consumption rate of the *hif-3a*$^{+/+}$ was even higher than that of the *hif-3a*$^{-/-}$ (Fig. 1E), indicating that the

oxygen consumption is not the cause. In order to validate the dissolved O_2 in water of the flasks is actually correlated with the O_2 concentration priorly adjusted in the Hypoxia workstation, we measured the dissolved O_2 in water with an LDO101 probe at different time points when the flasks were put into Hypoxia workstation set at 5% O_2 and 2% O_2 respectively (Fig. S2D, S2E). As expected, the dissolved O_2 in water with 2% O_2 setting was decreased faster than that with 5% O_2 setting, suggesting a precise correlation (Fig. S2D, S2E).

Thus, our data suggested that disruption of *hif-3a* attenuated hypoxia tolerance in zebrafish.

Disruption of hif-3a in zebrafish reduced erythrocytes

When we routinely examined the *hif-3a*$^{+/+}$ and *hif-3a*$^{-/-}$ larvae under a dissection microscope, we noticed that the *hif-3a*$^{-/-}$ larvae always had fewer blood cells compared to *hif-3a*$^{+/+}$ larvae. Given the importance of red blood cells for hypoxia tolerance (Bigham and Lee, 2014; Lee and Percy, 2011; Lorenzo et al., 2014; Sun et al., 2017), we measured the red blood cells of *hif-3a*$^{+/+}$ and *hif-3a*$^{-/-}$ embryos using O-dianisidine staining. At 36-hpf, there were fewer o-dianisidine-positive cells in the *hif-3a*$^{-/-}$ embryos than in the *hif-3a*$^{+/+}$ embryos (Fig. 2A, B). *Gata1* is an erythroid-specific transcription factor that is essential for erythropoiesis, and Tg(*gata1*:eGFP) zebrafish are widely used for monitoring living red blood cells (de Jong and Zon, 2005; Ferreira et al., 2005; Long et al., 1997; Lyons et al., 2002). To validate our observed phenotype, we mated Tg(*gata1*:eGFP) zebrafish with *hif-3a*$^{-/-}$, generating Tg(*gata1*:eGFP)/*hif-3a*$^{+/+}$ and Tg(*gata1*:eGFP)/*hif-3a*$^{-/-}$. From 24 - 48 hpf, we observed fewer *gata1*-positive cells in the *hif-3a* $^{-/-}$ than in their WT siblings (Fig. 2C, D). These data suggested that knockout of *hif-3a* disrupted erythropoiesis in zebrafish.

Reduced hypoxia tolerance was not only exhibited by the *hif-3a* $^{-/-}$ larvae (Fig. 1A, B, D), but also by the *hif-3a* $^{-/-}$ adults (Fig. 1C; Video S2). Thus, we examined erythrocyte numbers in adult. As it is difficult to measure total erythrocytes in each adult, we used relative erythrocyte number (the number of cells counted in a given blood volume) to compare *hif-3a* $^{+/+}$ and *hif-3a* $^{-/-}$ adults. Consistently, *hif-3a* $^{-/-}$ had fewer erythrocytes than *hif-3a* $^{+/+}$ (Fig. 2E).

To determine whether the defective erythropoiesis displayed by the *hif-3a*$^{-/-}$ was associated with erythroid maturation, we analyzed the morphology of isolated red blood cells using May-Grunwald-Giemsa staining (Fig. 2F, G) (De La Garza et al., 2016). *hif-3a* $^{-/-}$ had a higher percentage of proerythroblasts and a lower percentage of mature erythroid precursors at 2 dpf than the WT (Fig. 2F). The relative level of proerythroblasts decreased in the *hif-3a* $^{-/-}$ at 5 dpf, but remained higher than the level in their WT siblings (Fig. 2G). These data suggested that the deletion of *hif-3a* might impede erythroid cell maturation, resulted in

fewer mature red blood cells in *hif-3a* $^{-/-}$.

To determine whether loss of one copy of *hif-3a* can affect red blood cells and survival rate, we also compared the red blood cells among *hif-3a*$^{+/+}$, *hif-3a*$^{+/-}$ and *hif-3a*$^{-/-}$ embryos using O-dianisidine staining. No significant difference was detected between *hif-3a*$^{+/+}$and *hif-3a*$^{+/-}$ (Fig.S2F). In agreement with notion, under hypoxia, the death curve was similar between *hif-3a*$^{+/+}$and *hif-3a*$^{+/-}$ (Fig.S2G).

Disruption of zebrafish hif-3a abrogated the expression of hematopoietic marker genes and Ectopic expression of hif-3a mRNA rescued hematopoiesis defects in hif-3a $^{-/-}$ ***zebrafish***

To figure out the mechanisms of *hif-3a* on erythropoiesis, we examined the expression of hematopoietic markers using whole mount *in situ* hybridization. *scl* and *lmo2* are two primitive progenitor cell marker genes in zebrafish hematopoiesis (de Jong and Zon, 2005). At the 10-somite stage, no significant difference was detected in expression levels of *scl* and *lmo2* between *hif-3a* $^{+/+}$ and *hif-3a* $^{-/-}$ (Fig. S3A). *MyoD* staining (the somatic mesoderm marker) at the 14-somite stage indicated that overall embryogenesis was not influenced by disruption of *hif-3a* (Fig. S3B). However, at 24 hpf, *gata1* expression was dramatically reduced in *hif-3a* $^{-/-}$ embryos compared to *hif-3a* $^{+/+}$ embryos. Consistently, the expression levels of *alas2* (a key enzyme for heme biosynthesis) and *band3* (an erythroid-specific cytoskeletal protein) were reduced in *hif-3a* $^{-/-}$ at 24 hpf (Brownlie et al., 1998; Paw et al., 2003)(Fig.3A). In addition, the expression levels of *hbae1*, *hbae3* and *hbbe1* (three erythrocyte-specific hemoglobin genes), were reduced in *hif-3a* $^{-/-}$ at 48 hpf compared with those of *hif-3a* $^{+/+}$ (Fig. 3B). The downregulation of *gata1* expression in *hif-3a* $^{-/-}$ at 24 hpf was confirmed with quantitative RT-PCR assays (qRT-PCR) (Fig. S4A). The decreased expression levels of *alas2*, *band3*, *hbae1*, *hbae3* and *hbbe1* in *hif-3a* $^{-/-}$ as compared with *hif-3a* $^{+/+}$ were also confirmed by qRT-PCR assays (Fig. S4A, B).

Murine models suggest that *Runx1* and *c-myb* are important factors for adult erythropoiesis (Ferreira et al., 2005). Based on the erythrocyte reduction we observed in adult *hif-3a* $^{-/-}$, we sought to determine whether *runx1* and *c-myb* were also downregulated in adult *hif-3a*$^{-/-}$. Surprisingly, *runx1* and *c-myb* were upregulated, not downregulated, in the kidneys of adult *hif-3a* $^{-/-}$ compared with *hif-3a* $^{+/+}$ (Fig. S4C). These results suggested that *hif-3a* might not induce *runx1* and *c-myb* expression, and that the decreased erythrocytes in adult *hif-3a* $^{-/-}$ might not be due to the effects of *runx1* and *c-myb*.

The glycoprotein hormone erythropoietin (EPO), which is induced by HIF-α, regulates red blood cell mass, connecting the hypoxia signaling pathway with erythropoiesis (Lee and Percy, 2011). To determine whether *hif-3a* modulates adult erythropoiesis by regulating *epo*, similar to the behavior of *Hif-1a* and *Hif-2a*, we measured *epo* expression in adult zebrafish kidneys. Unexpectedly, *epo* expression was upregulated, not downregulated, in *hif-3a*$^{-/-}$ compared to *hif-3a*$^{+/+}$ (Fig. S4C). To further determine whether the modulation of erythropoiesis by *hif-3a* is indeed independent of Epo, we examined the effect of micro-injection of *epo* mRNA on erythropoiesis in *hif-3a*$^{-/-}$ embryos. Of note, micro-injection of *epo* mRNA could not rescue the defects of erythropoiesis in *hif-3a*$^{-/-}$ embryos (Fig.S5). These data suggested that *hif-3a* might not modulate erythropoiesis by directly regulating *epo* expression.

To further confirm that erythropoiesis defects of *hif-3a* $^{-/-}$ were specifically due to silencing of *hif-3a*, we microinjected synthesized *hif-3a* mRNA into *hif-3a* $^{-/-}$ embryos at the one-cell stage. Expression of microinjected *hif-3a* mRNA was confirmed (Fig. S6A). We then examined red blood cells using O-dianisidine staining, and quantified marker gene expression using whole mount *in situ* hybridization and qRT-PCR assays. At 36 hpf, embryos microinjected with *hif-3a* mRNA had more red blood cells than embryos microinjected with GFP-mRNA (Fig. 3C). Consistently, the expression levels of *gata1*, *alas2*, *band3*, *hbae1*, *hbae3* and *hbbe1* were higher in the *hif-3a* $^{-/-}$ embryos microinjected with *hif-3a* mRNA as compared with the *hif-3a*$^{-/-}$ embryos microinjected with GFP-mRNA (Fig. 3D, E; Fig. S6B, C).

These data suggested that the disruption of zebrafish *hif-3a* abrogated the expression of hematopoietic marker genes, resulted in defects of erythropoiesis; and that *gata-1* might be the downstream effector mediating the function of *hif-3a* in erythropoiesis.

Zebrafish have two waves of hematopoiesis, primitive hematopoiesis (embryonic hematopoiesis) and definitive hematopoiesis (adult hematopoiesis) (de Jong and Zon, 2005; Paik and Zon, 2010). *Gata1* is critical for both primitive erythropoiesis and definitive erythropoiesis (Ferreira et al., 2005). In this study, we found that *gata1* was downregulated in *hif-3α* $^{-/-}$, which correlated well with the reduction of erythrocytes in *hif-3α*$^{-/-}$. Therefore, *gata1* might be the main target by which *hif-3α* mediates erythropoiesis.

Hif-3a activated gata1 expression by recognizing the hypoxia-response element (HRE) site located in the gata1 promoter

While the function of mammalian *Hif-3a* is debatable due to the complexity of the splicing isoforms, zebrafish *hif-3a* serves as an oxygen-dependent transcription factor (Zhang et al., 2016). We observed that erythroid cell maturation was retarded, and *gata1* expression was reduced during erythropoiesis in *hif-3a* $^{-/-}$ zebrafish. Therefore, we attempted to determine whether zebrafish *hif-3a* acted as a transcription factor to regulate *gata1* expression. Initially, we examined expression patterns of *hif-3a* and *gata-1* in adult zebrafish tissues (3 mpf) as well as the different developmental stages. *hif-3a* was highly expressed in kidney, and *gata1* was highly expressed in spleen and kidney (Fig. 4A, B), indicating a correlation expression pattern between *hif-3a* and *gata-1* in tissues. Intriguingly, during development, *hif-3a* expression reached to the highest level from 12 to 16 hpf, *gata1* expression started to increase from 12 hpf and reached to the highest level at 16 hpf (Fig. 4C, D), further implicating an intrinsic connection between *hif-3a* and *gata-1* expression.

Subsequently, we examined whether *hif-3a* had transcriptional activity using an artificial luciferase reporter assay system in embryos (Zhou et al., 2009). Hif-3a indeed had transcriptional activity (Fig. 4E). Subsequently, we prepared a series of deletion and mutation constructs for the zebrafish *gata1* promoter luciferase reporter (Fig. 4F). Overexpression of *hif-3a* significantly activated the *gata1* promoter luciferase constructs, -1380 — +1580, -890 — +1580, -406 — +1580 and -164 — +1580 in EPC cells (Fig. 4G). However, when a potential HRE (GCGTG) located at -105 — -101 was mutated (GAAAG) (Fig. 4F), the promoter luciferase reporter (-406—+1580/HRE mutant) was not activated by overexpression of *hif-3a* in EPC cells (Fig. 4H). Further chromatin-immunoprecipitation assay (ChIP) using anti-hif-3a antibody (Zhang et al., 2012a) indicated that hif-3a could bind to the *gata-1* promoter containing HRE site (Fig. 4I).

In addition to *hif-3a/hif-3a1*, another splicing alternative isoform is known in zebrafish: *hif-3a*2 (Duan, 2016a; Zhang et al., 2016). Disruption of *hif-3a* at two loci also generated two novel peptides (M1 and M2) (Fig. S2B). To determine whether these three proteins affected *gata1* induction, we performed promoter assays. Interestingly, overexpression of these three proteins did not activate the *gata1* promoter (Fig. S7A-C). These findings not only suggested that *hif-3a/ hif-3a*1 plays a specific role for *gata1* induction, but also indicated that the knockout of *hif-3a* at two loci completely disrupted *hif-3a* function in zebrafish.

In the mutant M2 (*hif-3a*$^{ihb20180621/ihb20180621}$), we confirmed that the expression levels of *gata1*, *alas2*, *hbae1* and *hbbe1* were reduced compared with WT siblings (*hif-3a*$^{+/+}$) (Fig. S8A, B). Thus, our results suggested that zebrafish *hif-3a* directly activated *gata1* expression by recognizing the HRE site located in the promoter of

gata1.

Whether HIF-3α acts as a dominant negative transcriptional regulator of HIF-1α and/or HIF-2α, or acts as a transcription factor in response to hypoxia is largely dependent upon the variant and the biological model, particularly in mammalian (Heikkila et al., 2011; Makino et al., 2007; Maynard et al., 2005). However, in zebrafish, hif-3α binds to the promoter sequences of several genes, and induces the expression of these genes under hypoxic conditions (Zhang et al., 2014). Here, we provided additional evidence supporting that zebrafish *hif-3α* serves as a transcription factor to induce *gata1* expression.

As reported previously, hif-3α is degraded during normoxia in zebrafish (Zhang et al., 2014). However, in this study, we observed that defects of erythropoiesis in *hif-3a* $^{-/-}$ zebrafish were steady-state. We sought to determine whether hif-3a protein stability was also steady-state from embryos to adult tissues. By Western blot analysis, we confirmed hif-3α protein was stable from embryos to adult tissues (Fig. S1E and S9).

In addition, we noticed that disruption of *hif-3α* enhanced expression of *hif-1αb* and *hif-2αb*, suggesting some redundant functions between *hif-3α and hif-1α/hif-2α* in zebrafish (Fig. S10A and S10B). In consistent with this notion, the *hif-1a* down-stream targets *glut1*, *pdk1*, and the *hif-2a* down-stream targets *pou5f1*, *pai1* were increased in *hif-3a*$^{-/-}$ larvae (Fig. S10C-S10F).

Given the well-known role of *hif-1a* in regulating erythropoiesis (Semenza, 2009), we intended to determine whether microinjection of *hif-1αb* mRNA could rescue the defects of erythropoiesis in *hif-3a*$^{-/-}$ embryos. Base on O-dianisidine staining of embryos, microinjection of *hif-1αb* mRNA could partially restore the defects of erythropoiesis in *hif-3a*$^{-/-}$ embryos (Fig. S10G-S10I). Furthermore, we found that the red blood cell numbers were partially recovered and their maturation was obviously fixed after microinjection of *hif-1αb* mRNA (Fig.S10J-S10M), which seemed to rely on *gata1* upregulation because *gata1* expression was indeed increased (Fig.S10N and S10O).

In this study, we noticed that disruption of *hif-3α* could cause redundant upregulation of *hif-1ab*. It appeared that microinjection of *hif-1αb* mRNA could induce *gata1* upregulation, resulting in partially rescuing defects of erythropoiesis in *hif-3a*$^{-/-}$ embryos. However, disruption of *hif-3α* in zebrafish eventually caused defects of erythropoiesis. Therefore, the direct upregulation of *gata1* by *hif-3α* might account for a main mechanism of *hif-3α* in modulating erythropoiesis of zebrafish.

Given the well-known role of PHD enzymes and VHL protein in regulating HIF activity and the similarity among HIF-1α, HIF-2α and HIF-3α, we sought to determine whether zebrafish *phd2a*, *phd2b*, *phd3* and *vhl* have effects on *hif-3α* activity. We performed promoter assays and Western blot analysis. Co-expression of

phd2a, *phd2b*, *phd3* and *vhl* decreased the activity of HRE luciferase reporter and *gata-1* promoter reporter induced by *hif-3α* (Fig. S11A and S11B). As expected, co-expression of *phd2a*, *phd2b*, *phd3* and *vhl* also caused hif-3α protein degradation. These data suggested that *hif-3α* might behave similar to *hif-1α* and *hif-2α* in hypoxia signaling pathway.

MATERIALS AND METHODS

Generation of hif-3a-null zebrafish

We used CRISPR/Cas9 to knockout *hif-3a* in zebrafish. First, *hif-3a* sgRNA was designed using the CRISPR design tool (http://crispr.mit.edu). The zebrafish codon Optimized Cas9 plasmid was digested with XbaI, then purified and transcribed using the T7 mMessage mMachine Kit (Ambion). We used a PUC9 gRNA vector to amplify *hif-3a* sgRNA template. The primers used to amplify *hif-3a* sgRNA were as follows: forward primer 1 (mutant 1) (5'-GTAATACGACTCACTATAGGAC AAAGCTGCCATCATGAGTTTTAGAGCTAGAAATAGC-3'); forward primer 2 (mutant 2) (5'-GTA ATACGACTCACTATAGGTGGTGTTATTTCACTCTGGTTTTAGAGCTAGAAATAGC-3'); and the reverse primer (5'-AAAAGCACCGACTCGGTGCC-3'). SgRNA was synthesized using the Transcript Aid T7 High Yield Transcription Kit (Fermentas).

We injected zebrafish embryos at one-cell stage (generated as described above) with 1 ng Cas9 RNA and 0.15 ng sgRNA per embryo. The mutations were initially detected using a HMA as previously described(Cai et al., 2018). If the HMA results were positive, the remaining embryos were raised to adulthood as the F0 generation, and were then backcrossed with WT zebrafish (strain AB) to generate the F1 generation. F1s were genotyped with HMAs. Genetype was confirmed by sequencing target sites. Heterozygous F1s were back-crossed with WT zebrafish (strain AB; disallowing offspring-parent matings) to generate the F2 generation. F2 adults carrying the target mutation were inter-crossed to generate F3 offspring. The F3 generation contained WT (+/+), heterozygous (+/-) and homozygous (-/-) individuals. The primers used to identify mutants were as follows: forward primer 1 (the mutant 1) (5'-AGTTTGGAGCAGCGGAAG-3'); reverse primer 1 (the mutant 1) (5'-AGCATTAGGACATTATGCAGGT-3'); forward primer 2 (the mutant 2) (5'-CGAAAGGACAGTCAGAGGTAGA-3'); and reverse primer 2 (the mutant 2) (5'-ACCGTTTCCTAGAATTACTGGTTAG-3'). The two novel mutants were named following zebrafish nomenclature guidelines, *hif-3a*$^{ihb20180620/ihb20180620}$(http://zfin.org/ZDB-ALT-180620-1), and *hif-3a*$^{ihb20180621/ihb20180621}$(http://zfin.org/ZDB-ALT-180620-2).

Zebrafish maintenance and cell culture

Zebrafish (Danio rerio) strain AB, as well as the transgenic line Tg(gata1:EGFP) (provided by Tingxi Liu) were raised, maintained and staged according to standard protocols. Epithelioma papulosum cyprini (EPC) cells originally obtained from ATCC (American Type Culture Collection, Manassas, VA, USA) were cultured in M199 medium supplemented with 10% fetal bovine serum, maintained at 28℃ in a humidified incubator containing 5% CO2. EPC cells were transfected with the constructed plasmids using VigoFect (Vigorous Biotechnology, Beijing, China) following the manufacturer's instruction. pTK-Renilla (Promega) was used as an internal control. After transfection, the luciferase activity was measured with the dual-luciferase reporter assay kit following the manufacture's instruction (Promega).

Hypoxia treatment

The Ruskinn Invivo2 I-400 workstation was used for hypoxia treatment of zebrafish (larvae and adults). The O_2 concentration was adjusted to the appropriate value (2% for larvae and 5% for adults) prior to experimentation. In our previous studies, we noted that the body weight of adult zebrafish significantly affected hypoxia tolerance (Cai et al., 2018). Therefore, we selected adult zebrafish (at 3 and 6 mpf) with similar body weights (0.32 ± 0.02g ; 0.65 ± 0.02g) for the tests of hypoxia tolerance.

For the hypoxia treatments of zebrafish larvae, *hif-3a*-null and WT zebrafish were placed into a 10 cm cell culture dish filled with 30 ml of water. The oxygen concentration in the Ruskinn INVIVO2 I-400 workstation was adjusted to 2% ahead of time. Each experiments was repeated three times.

Whole mount in situ hybridization and O-dianisidine staining

Whole mount in situ hybridization (WISH) was performed as described previously (Hu et al., 2014). Probes for *scl*, *lmo2*, *gata1*, *myoD*, *alas2*, *band3*, *hbae1*, *hbae3* and *hbbe1* were amplified from the cDNA pool using the primers.

O-dianisidine staining for hemoglobin was performed as previously described (Hu et al., 2014). Live embryos were soaked in O-dianisidine staining solution (0.6mg/mL O-dianisidine, 166ul 3M ammonium acetate, 20ml absolute ethyl alcohol, 30ml ddH_2O) for 15minutes in the dark.

The software IpWin32 was used for quantifying the erythrocyte numbers, GFP-positive cells numbers and genes expression levels in WISH staining. The cells numbers and gene expression levels were measured from the field with a same square and different larvae was chosen for counting (n=3).

Luciferase reporter assays and transcriptional activity assays

EPC cells were seeded in 24-well plates and transfected with the indicated plasmids together with zebrafish *gata1* promoter luciferase reporters and pTK-Renilla as an internal control. Luciferase activity was measured 20–24h after transfection using the Dual-luciferase Reporter Assay System (Promega). For embryos, the plasmids were injected into the embryos at the one-cell stage. About 30 embryos were harvested at 10hpf and homogenized in Passive Lysis Buffer (Promega). Each experiment was conducted in triplicate and repeated at least three times.

May–Grunwald–Giemsa staining

The embryos (2dpf and 5 dpf, respectively) were placed in 1X PBS dropped on glass slides. The blood cells were released by puncturing the pericardial sac and upper yolk sac of embryos with a fine forcep. The slides were air dried at room temperature before staining. The blood cells were stained with May–Grunwald-Giemsa solution 1 (ServiceBio) (100µl) for 5 minutes and briefly rinsed in purified water, and then stained with May–Grunwald-Giemsa solution 2 (200µl) for 10 minutes and briefly rinsed with purified H_2O. Once the slides were dry, a drop of neutral resin was added. Subsequently, the slides were covered with slips and dried overnight. The stained blood cells were visualized and photographed under a 100X oil-immersion lens.

Erythrocyte number counting in adult zebrafish (6mpf)

Adult zebrafish (n=3 for *hif-3a*$^{+/+}$ and *hif-3a*$^{-/-}$ respectively; 6mpf; body weight=0.63±0.01g) were skin-dried carefully by filter paper and dissected near to heart region using an eye scissor. Approximately 15µL blood was collected from the beating heart using a syringe infiltrated with heparin in advance. Subsequently, 1µL blood was mixed with 99µL phosphate-buffered saline (PBS) in 1.5mL EP tube. 10µL diluted blood was added into a hemacytometer for counting the erythrocyte number. The erythrocytes in 10 chambers (1mm×1mm) were counted under an invert microscope for each zebrafish. Each zebrafish was counted for three times in different field randomly. Simultaneously, the blood cell pictures were photographed for reference.

Quantitative real-time PCR

Total RNAs were extracted from embryos or kidneys with TRIzol reagent (Invitrogen). The first-strand cDNA synthesis kit (Fermentas) to synthesize cDNA. Quantitative RT-PCR assays were performed using MonAmp™ SYBR® Green qPCR Mix (high Rox) (Monad Bio., Shanghai, China). The primers used for RT-PCR were as follows: *hif-3a*: 5'- GCTGGATGGCTTGTCTGATGG -3' and 5'-CCCTCATGAGAGCTGCTGTG -3'; *gata-1*: 5'- GAGACTGACCTACTGCCATCG -3' and 5'-TCCCAGAATTGACTGAGATGAG -3'; *alas2*: 5'- GCAAAATGGCCTTCTCCCTC -3' and 5'-TCAAACCTGAGGTGTCTTGG -3'; *band3*: 5'- GTGATGGTTGGTGTCTCAAT -3 'and 5'-TAGTTGGCACACGGGTGACA -3'; *hbae1*: 5'- CTCTCTCCAGGATGTTGATT -3' and 5'-GGGACAGAATCTTGAAATTG -3' *hbae3*: 5'- CTCTTTCCAGGACTTTGTTC -3' and 5'-GGTTGATGATCTTGAAGTTT -3' *hbbe1*: 5'- ATGGTTGCTGCCCACGGTAA -3' and 5'-CAGCCAAAAGCCTGAAGTTG -3' *β-actin*: 5'- TACAATGAGCTCCGTGTTGC -3' and 5'-ACATACAATGGCAGGGGTGTT -3'; *runx*: 5'- GGGACGCCAAATACGAACCT-3' and 5'-GCAGGACGGAGCAGAGGAAG-3'; *c-myb*: 5'-AGTTACTTCCGGGAAGAACCG-3' and *c-myb*: 5'-AGAGCAAGTGGAAATGGCACC-3'; *epo*: 5'-GTGCCTCTCACTGAGTTCTTGGAAG -3' and 5'-CTCGTTCAGCATGTGTAAGCCTGAC-3'. *β-actin* was used as internal controls. Applied Biosystems Step One was used for data collection.

Oxygen concentration measurement

We measured zebrafish oxygen consumption in 250-ml flasks (n=12), each containing 250 ml water. The oxygen concentration in water was measured with an LDO101 probe (HQ30d, HACH). The total 12 adult zebrafish with similar weight (n=6 for *hif3a*-null and WT respectively) were used for measurement. We placed each *hif3a*-null or WT zebrafish in individual flask, and then tightly sealed the flasks with plastic film. After 4 h, we measured the oxygen concentration in flasks (n=6) with the LDO101 probe individually. After 8 h, we measured the oxygen concentration in the remaining flasks (n=6) with the LDO101 probe individually.

Chromatin-immunoprecipitation (ChIP) assay

We performed ChIP assays using an Enzymatic Chromatin IP Kit (9002s) (Cell Signaling Technology) following the protocol provided by the manufacture. Briefly, 2000 embryos were harvested at 16 hpf and sonicated. Then, the protein A/G agarose beads (30 μl) (Santa Cruz) were added to each sample and the

mixtures were rotated at 4℃ for 1 h. Subsequently, the supernatants were incubated with anti-hif-3a antibody (provided by Dr. Cunming Duan)(Zhang et al., 2012a) or rabbit IgG (control) (Santa Cruz) respectively and rotated at 4℃ overnight. The primers for amplifying the promoter region of *gata1* was as follow: 5'-GTCTATAAGGTCATATAG GC-3'and 5'-CTTCAGTCTTTGGGAACTAG-3'. The primers for amplifying *β-actin* was as follow: 5'-ATCATGTTCGAGACCTTCAA-3' and 5'-TAGCTCTTCTCCAGGGAGGA-3'.

Erythrocyte number counting in adult zebrafish and quantification of RNA levels in zebrafish embryos

We used Image-Pro Plus software to analyze digital images for counting erythrocyte numbers and quantifying RNA levels. For counting erythrocyte numbers, briefly, a standard color parameter of one cell was set and the rectangular AOI was used to select region, then, the IOD parameter was chosen for measuring the signal. For quantifying RNA levels of *in situ* hybridization staining, the RNA signal measured from *in situ* hybridization staining of one control zebrafish was set as "1" initially, the RNA levels in other zebrafish were calculated after compared with the signal value of control zebrafish.

Erythrocyte number counting in zebrafish larvae (2dpf)

The zebrafish larvae (2dpf) were placed in 10 μL 1 × PBS dropped on glass slides. The blood cells were released by puncturing the pericardial sac and upper yolk sac of embryos with a fine forcep. Then mixed with 90-μL PBS in 1.5 mL EP tube. 10-μL diluted blood was added into a hemocytometer for counting the erythrocyte number. The erythrocytes in 4 chambers (1mm × 1mm) were counted under an invert microscope for each zebrafish (n=5 larvae). Each zebrafish was counted for three times in different field randomly. Simultaneously, the blood cell pictures were photographed for reference.

Statistical analysis

GraphPad Prism 7 software (GraphPad Software, San Diego, CA) was used for all statistical analysis. Differences between experimental and control groups were determined by unpaired two-tailed Student's t test (where two groups of data were compared). P values less than 0.05 were considered statistically significant. For animal survival analysis, the Kaplan–Meier method was adopted to generate graphs, and the survival curves were analyzed by log-rank analysis.

Supplementary Data

Supplementary Data contain Supplementary Video S1, Supplementary Video S2 and Supplementary 11 Figures.

Acknowledgements

We are grateful to Drs. Cunming Duan and Ling Lu for providing anti-hif-3α antibody. We also thank Drs. Peter Ratcliffe, Navdeep Chandel, Bo Zhang and Jingwei Xiong for the generous gift of reagents.

Competing interests

The authors declare no competing or financial interests.

Author contributions

Conceptualization: W.X., X.C.; Methodology: X.C.; Validation: X.C., Z.Z., J.Z.; Formal analysis: W.X., X.C.; Investigation: W.X., X.C., Z.Z.; J. Z.; Resources: J.Z., D.Z., Q.L., X.L., J.W., G.O.; Data curation: Z.Z., J. Z., D.Z.; Writing-original draft: W.X., X.C.; Writing-review & editing: W.X., X.C.; Visualization: X.C., Z.Z.; Supervision: W.X.; Funding acquisition: W.X.

Funding

W. X. is supported by the Strategic Priority Research Program of the Chinese Academy of Sciences Grant XDA24010308; NSFC grant numbers 31830101, 31721005 and 31671315; and National Key R & D Program of China 2018YFD0900602. X. C. is supported by State Key Laboratory of Freshwater Ecology and Biotechnology Grant 2020FB07.

Supplementary information

Supplementary data contain Supplementary Video S1, Video S2 and Supplementary 11 Figures

References

Aragones, J., Fraisl, P., Baes, M. and Carmeliet, P. (2009). Oxygen sensors at the crossroad of metabolism. *Cell metabolism* **9**, 11-22.

Augstein, A., Poitz, D. M., Braun-Dullaeus, R. C., Strasser, R. H. and Schmeisser, A. (2011). Cell-specific and hypoxia-dependent regulation of human HIF-3alpha: inhibition of the expression of HIF target genes in vascular cells. *Cellular and molecular life sciences : CMLS* **68**, 2627-2642.

Bigham, A. W. and Lee, F. S. (2014). Human high-altitude adaptation: forward genetics meets the HIF pathway. *Genes Dev* **28**, 2189-2204.

Bishop, T. and Ratcliffe, P. J. (2015). HIF hydroxylase pathways in cardiovascular physiology and medicine. *Circ Res* **117**, 65-79.

Brownlie, A., Donovan, A., Pratt, S. J., Paw, B. H., Oates, A. C., Brugnara, C., Witkowska, H. E., Sassa, S. and Zon, L. I. (1998). Positional cloning of the zebrafish sauternes gene: a model for congenital sideroblastic anaemia. *Nature genetics* **20**, 244-250.

Cai, X., Zhang, D., Wang, J., Liu, X., Ouyang, G. and Xiao, W. (2018). Deletion of the fih gene encoding an inhibitor of hypoxia-inducible factors increases hypoxia tolerance in zebrafish. *The Journal of biological chemistry* **293**, 15370-15380.

de Jong, J. L. O. and Zon, L. I. (2005). Use of the zebrafish system to study primitive and definitive hematopoiesis. *Annu Rev Genet* **39**, 481-501.

De La Garza, A., Cameron, R. C., Nik, S., Payne, S. G. and Bowman, T. V. (2016). Spliceosomal component Sf3b1 is essential for hematopoietic differentiation in zebrafish. *Experimental hematology* **44**, 826-837 e824.

Duan, C. (2016a). Hypoxia-inducible factor 3 biology: complexities and emerging themes. *Am J Physiol Cell Physiol* **310**, C260-269.

Duan, C. M. (2016b). Hypoxia-inducible factor 3 biology: complexities and emerging themes. *Am J Physiol-Cell Ph* **310**, C260-C269.

Ferreira, R., Ohneda, K., Yamamoto, M. and Philipsen, S. (2005). GATA1 function, a paradigm for transcription factors in hematopoiesis. *Mol Cell Biol* **25**, 1215-1227.

Greer, S. N., Metcalf, J. L., Wang, Y. and Ohh, M. (2012). The updated biology of hypoxia-inducible factor. *Embo J* **31**, 2448-2460.

Gu, Y. Z., Moran, S. M., Hogenesch, J. B., Wartman, L. and Bradfield, C. A. (1998). Molecular characterization and chromosomal localization of a third alpha-class hypoxia inducible factor subunit, HIF3 alpha. *Gene Expression* **7**, 205-213.

Hara, S., Hamada, J., Kobayashi, C., Kondo, Y. and Imura, N. (2001). Expression and characterization of hypoxia-inducible factor (HIF)-3alpha in human kidney: suppression of HIF-mediated gene expression by HIF-3alpha. *Biochem Biophys Res Commun* **287**, 808-813.

Heikkila, M., Pasanen, A., Kivirikko, K. I. and Myllyharju, J. (2011). Roles of the human hypoxia-inducible factor (HIF)-3alpha variants in the hypoxia response. *Cellular and molecular life sciences : CMLS* **68**, 3885-3901.

Hu, B., Zhang, W., Feng, X., Ji, W., Xie, X. and Xiao, W. (2014). Zebrafish eaf1 suppresses foxo3b expression to modulate transcriptional activity of gata1 and spi1 in primitive hematopoiesis. *Dev Biol* **388**, 81-93.

Lee, F. S. and Percy, M. J. (2011). The HIF pathway and erythrocytosis. *Annual review of pathology* **6**, 165-192.

Long, Q. M., Meng, A. M., Wang, H., Jessen, J. R., Farrell, M. J. and Lin, S. (1997). GATA-1 expression pattern can be recapitulated in living transgenic zebrafish using GFP reporter gene. *Development* **124**, 4105-4111.

Lorenzo, F. R., Huff, C., Myllymaki, M., Olenchock, B., Swierczek, S., Tashi, T., Gordeuk, V., Wuren, T., Ri-Li, G., McClain, D. A., et al. (2014). A genetic mechanism for Tibetan high-altitude adaptation. *Nature genetics* **46**, 951-+.

Lyons, S. E., Lawson, N. D., Lei, L., Bennett, P. E., Weinstein, B. M. and Liu, P. P. (2002). A nonsense mutation in zebrafish gata1 causes the bloodless phenotype in vlad tepes. *Proc Natl Acad Sci U S A* **99**, 5454-5459.

Majmundar, A. J., Wong, W. J. and Simon, M. C. (2010). Hypoxia-inducible factors and the response to hypoxic stress. *Mol Cell* **40**, 294-309.

Makino, Y., Cao, R., Svensson, K., Bertilsson, G., Asman, M., Tanaka, H., Cao, Y., Berkenstam, A. and Poellinger, L. (2001). Inhibitory PAS domain protein is a negative regulator of hypoxia-inducible gene expression. *Nature* **414**, 550-554.

Makino, Y., Uenishi, R., Okamoto, K., Isoe, T., Hosono, O., Tanaka, H., Kanopka, A., Poellinger, L., Haneda, M. and Morimoto, C. (2007). Transcriptional up-regulation of inhibitory PAS domain protein gene expression by hypoxia-inducible factor 1 (HIF-1): a negative feedback regulatory circuit in HIF-1-mediated signaling in hypoxic cells. *J Biol Chem* **282**, 14073-14082.

Maynard, M. A., Evans, A. J., Hosomi, T., Hara, S., Jewett, M. A. and Ohh, M. (2005). Human HIF-3alpha4 is a dominant-negative regulator of HIF-1 and is down-regulated in renal cell carcinoma. *FASEB J* **19**, 1396-1406.

Maynard, M. A., Qi, H., Chung, J., Lee, E. H., Kondo, Y., Hara, S., Conaway, R. C., Conaway, J. W. and Ohh, M. (2003). Multiple splice variants of the human HIF-3 alpha locus are targets of the von Hippel-Lindau E3 ubiquitin ligase complex. *J Biol Chem* **278**, 11032-11040.

Paik, E. J. and Zon, L. I. (2010). Hematopoietic development in the zebrafish. *Int J Dev Biol* **54**, 1127-1137.

Pasanen, A., Heikkila, M., Rautavuoma, K., Hirsila, M., Kivirikko, K. I. and Myllyharju, J. (2010). Hypoxia-inducible factor (HIF)-3a is subject to extensive alternative splicing in human tissues and cancer cells and is regulated by HIF-1 but not HIF-2. *Int J Biochem Cell B* **42**, 1189-1200.

Paw, B. H., Davidson, A. J., Zhou, Y., Li, R., Pratt, S. J., Lee, C., Trede, N. S., Brownlie, A., Donovan, A., Liao, E. C., et al. (2003). Cell-specific mitotic defect and dyserythropoiesis associated with erythroid band 3 deficiency. *Nature genetics* **34**, 59-64.

Prabhakar, N. R. and Semenza, G. L. (2012). Adaptive and maladaptive cardiorespiratory responses to continuous and intermittent hypoxia mediated by hypoxia-inducible factors 1 and 2. *Physiological reviews* **92**, 967-1003.

---- (2015). Oxygen Sensing and Homeostasis. *Physiology (Bethesda)* **30**, 340-348.

---- (2016). Regulation of carotid body oxygen sensing by hypoxia-inducible factors. *Pflugers Arch* **468**, 71-75.

Ravenna, L., Salvatori, L. and Russo, M. A. (2016). HIF3alpha: the little we know. *FEBS J* **283**, 993-1003.

Semenza, G. L. (2009). Involvement of oxygen-sensing pathways in physiologic and pathologic erythropoiesis. *Blood* **114**, 2015-2019.

---- (2012). Hypoxia-inducible factors in physiology and medicine. *Cell* **148**, 399-408.

---- (2014). Oxygen sensing, hypoxia-inducible factors, and disease pathophysiology. *Annu Rev Pathol* **9**, 47-71.

Shen, C. and Kaelin, W. G., Jr. (2013). The VHL/HIF axis in clear cell renal carcinoma. *Semin Cancer Biol* **23**, 18-25.

Sun, K., Liu, H., Song, A., Manalo, J. M., D'Alessandro, A., Hansen, K. C., Kellems, R. E., Eltzschig, H. K., Blackburn, M. R., Roach, R. C., et al. (2017). Erythrocyte purinergic signaling components underlie hypoxia adaptation. *J Appl Physiol (1985)* **123**, 951-956.

Yamashita, T., Ohneda, O., Nagano, M., Iemitsu, M., Makino, Y., Tanaka, H., Miyauchi, T., Goto, K., Ohneda, K., Fujii-Kuriyama, Y., et al. (2008). Abnormal heart development and lung remodeling in mice lacking the hypoxia-inducible factor-related basic helix-loop-helix PAS protein NEPAS. *Mol Cell Biol* **28**, 1285-1297.

Zhang, P., Bai, Y., Lu, L., Li, Y. and Duan, C. (2016). An oxygen-insensitive Hif-3alpha isoform inhibits Wnt signaling by destabilizing the nuclear beta-catenin complex. *eLife* **5**.

Zhang, P., Lu, L., Yao, Q., Li, Y., Zhou, J., Liu, Y. and Duan, C. (2012a). Molecular, functional, and gene expression analysis of zebrafish hypoxia-inducible factor-3alpha. *Am J Physiol Regul Integr Comp Physiol* **303**, R1165-1174.

Zhang, P., Lu, L., Yao, Q., Li, Y., Zhou, J. F., Liu, Y. Z. and Duan, C. M. (2012b). Molecular, functional, and gene expression analysis of zebrafish hypoxia-inducible factor-3 alpha. *Am J Physiol-Reg I* **303**, R1165-R1174.

Zhang, P., Yao, Q., Lu, L., Li, Y., Chen, P. J. and Duan, C. M. (2014). Hypoxia-Inducible Factor 3 Is an Oxygen-Dependent Transcription Activator and Regulates a Distinct Transcriptional Response to Hypoxia. *Cell Reports* **6**, 1110-1121.

Zhou, J. G., Feng, X., Ban, B., Liu, J. X., Wang, Z. and Xiao, W. H. (2009). Elongation Factor ELL (Eleven-Nineteen Lysine-rich Leukemia) Acts as a Transcription Factor for Direct Thrombospondin-1 Regulation. *J Biol Chem* **284**, 19142-19152.

Zhou, X., Guo, X., Chen, M., Xie, C. and Jiang, J. (2018). HIF-3alpha Promotes Metastatic Phenotypes in Pancreatic Cancer by Transcriptional Regulation of the RhoC-ROCK1 Signaling Pathway. *Molecular cancer research : MCR* **16**, 124-134.

Figures

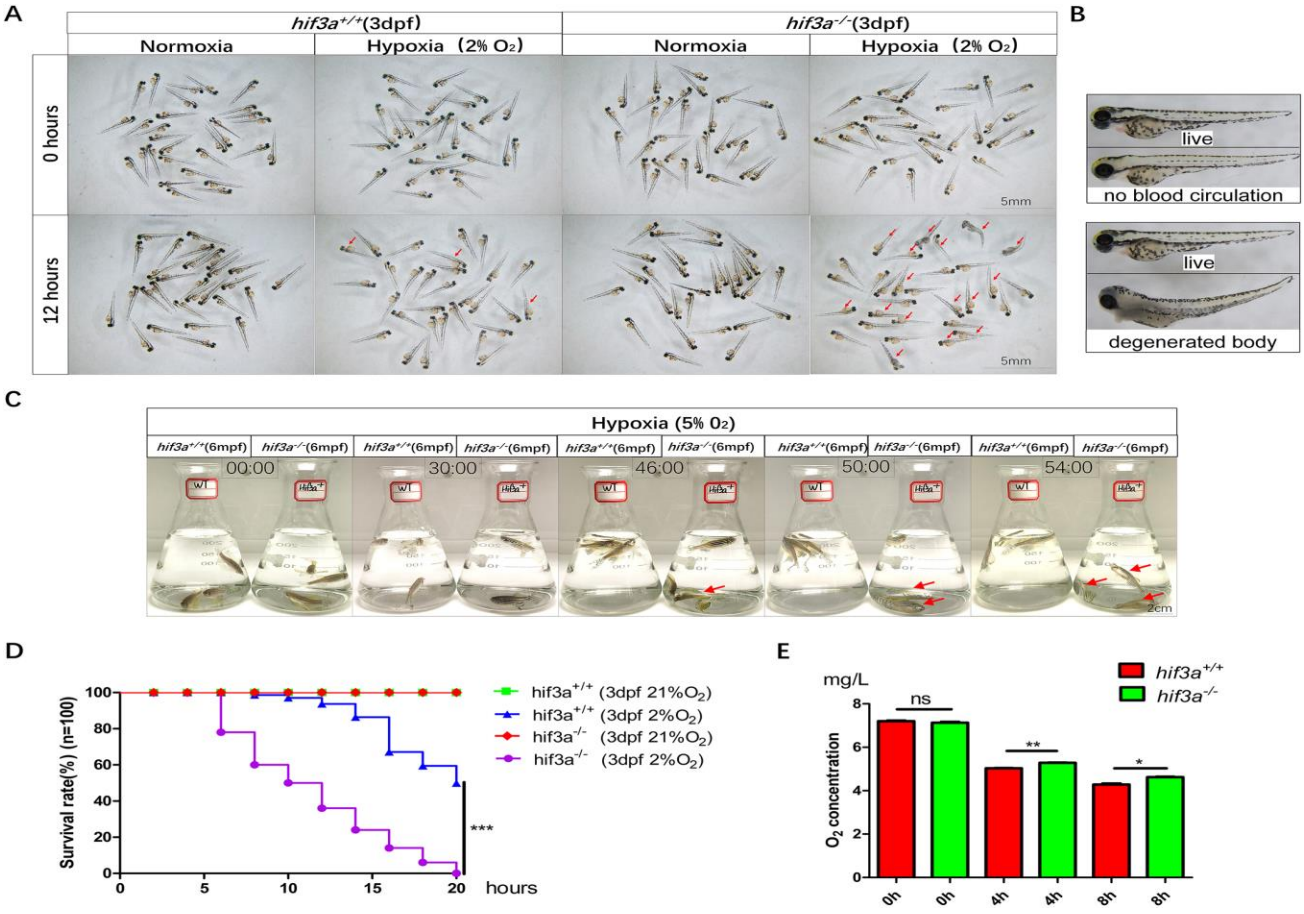

Figure 1. Zebrafish *hif-3a* facilitates hypoxia tolerance. (A) Representative images of *hif-3a*$^{-/-}$ larvae and WT (*hif-3*$^{+/+}$) larvae (30 larvae for each, 90 larvae in total; 3 dpf), subjected to normoxia (21% O_2) or hypoxia (2% O_2) for 12 h. The dead larvae (marked by red arrows) exhibited lack of movement, absence of blood circulation, and a bodily degeneration. (B) Representative images of living and dead zebrafish larvae. (C) *Hif-3a*$^{-/-}$ adults were more sensitive to hypoxia (5% O_2) as compared with their wild-type siblings. Survival of *hif-3a*$^{+/+}$ (left flask) and *hif-3a*$^{-/-}$ (right flask) (6 mpf) after 0 min, 30 min, 46 min, 50 min, and 54 min in hypoxic conditions (5% O_2) (3 zebrafish for each, 3 replicates). Red arrows indicate dying zebrafish. (D) The survival rate curve of *hif-3a*$^{-/-}$ larvae and their WT siblings. The oxygen concentration of the hypoxia workstation (Ruskinn INVIVO2 400) was adjusted to 2% prior to experimentation. The dead larvae were counted once every two hours (100 larvae). (E) Oxygen consumption rate was lower in *hif-3a*$^{-/-}$ than in their WT siblings (6 mpf). The experiments were repeated at least 3 times. dpf, days post-fertilization; mpf, months post-fertilization. Error bars indicate the standard error of the mean (S.E.M.); ns, not significant; * $p < 0.05$; ** $p < 0.01$; *** $p < 0.001$.

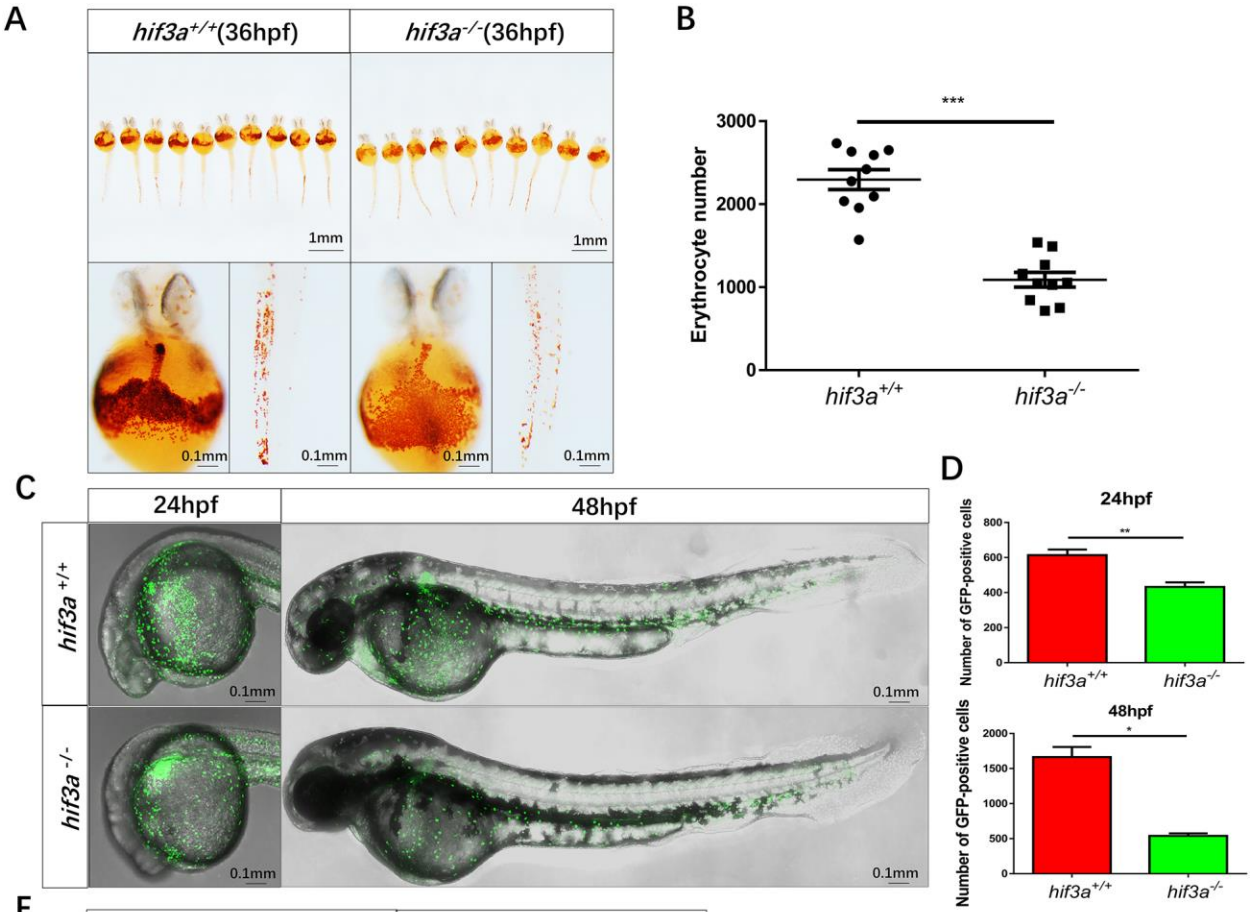

2dpf	Proerythroblast	Basophilic erythroblast	Orthochromatophilic erythroblast
hif3a$^{+/+}$	5 (4%)	65 (52%)	56 (44%)
hif3a$^{-/-}$	85 (56%)	35 (23%)	31 (21%)

5dpf	Proerythroblast	Basophilic erythroblast	Orthochromatophilic erythroblast
hif3a$^{+/+}$	4 (4%)	15 (13%)	109 (83%)
hif3a$^{-/-}$	18 (12%)	51 (33%)	85 (55%)

Figure 2. The number of erythrocytes is reduced and the primitive erythroid maturation is retarded in *hif-3a*$^{-/-}$. (A) O-dianisidine staining of functional hemoglobin in the mature primitive erythrocytes in *hif-3a*$^{+/+}$ (left) and *hif-3a*$^{-/-}$ (right) at 36 hpf. The experiments were repeated 3 times. (B) The number of erythrocytes was reduced in *hif-3a*$^{-/-}$ (10 larvae). (C) Fluorescent images of Tg(*gata1*:eGFP)/*hif-3a*$^{+/+}$ (top) and Tg(*gata1*:eGFP)/*hif-3a*$^{-/-}$ (bottom) indicated that *hif-3a*$^{-/-}$ have fewer *gata1*-positive erythrocytes at 24 hpf and 48 hpf. (D) Quantitation of *gata1*-positive erythrocytes in Tg(*gata1*:eGFP)/*hif-3a*$^{+/+}$ and Tg(*gata1*:eGFP)/*hif-3a*$^{-/-}$ at 24 hpf (up) and 48 hpf (down) (10 larvae for each, 3 replicates). (E) The number of erythrocytes was significantly reduced in *hif-3a*$^{-/-}$ compared to *hif-3a*$^{+/+}$ at 6 mpf. Representative image of erythrocytes in the counting chamber (1 mm×1 mm) (right); scatter plot indicates erythrocyte numbers in 10 counting chambers. (F, G) Representative images of May–Grunwald–Giemsa-stained erythroblasts in *hif-3a*$^{+/+}$ and *hif-3a*$^{-/-}$ larvae at 2 dpf (F) and 5 dpf (G). The percentages of cells were morphologically classified at various stages of maturation. Percentages of *hif-3a*$^{+/+}$ and *hif-3a*$^{-/-}$ larvae are shown in brackets. hpf, hours post-fertilization; dpf, days post-fertilization; mpf, months post-fertilization. Error bars indicate the standard error of the mean (S.E.M.); *$p < 0.05$; ** $p < 0.01$; ***$p < 0.001$.

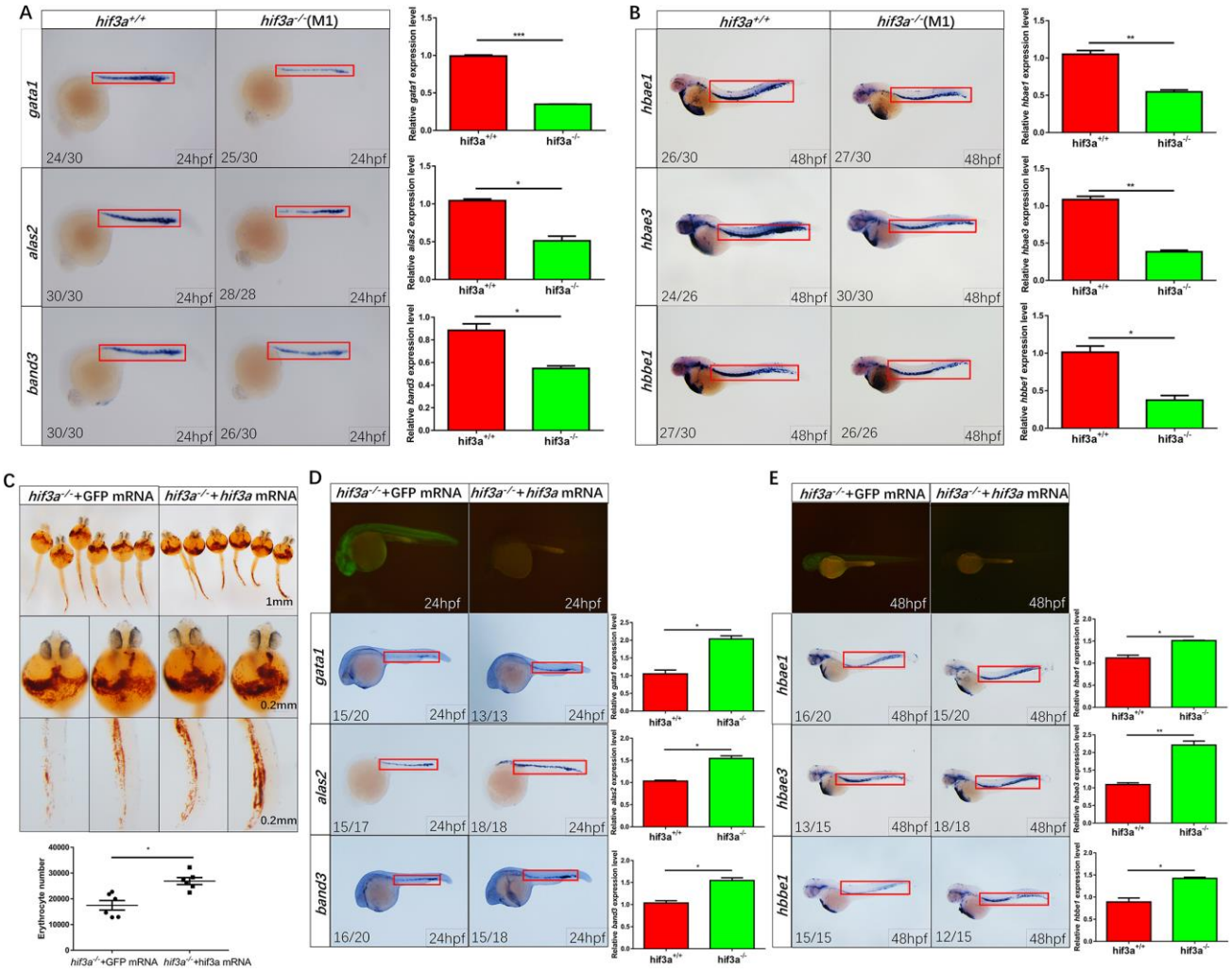

Figure 3. Disruption of *hif-3a* influences expression of hematopoietic marker genes, but ectopic expression of *hif-3a* partially rescues hematopoietic defects exhibited in *hif-3a*$^{-/-}$. (A) Expression levels of the erythrocytic markers *gata1*, *alas2*, and *band3* were reduced significantly in *hif-3a*$^{-/-}$ larvae at 24 hpf. Quantitation of the signal in red rectangle showed at the right panel (10 larvae for each, 3 replicates). (B) Expression levels of the erythrocyte-specific hemoglobin markers *hbae1*, *hbae3*, and *hbbe1* were reduced in *hif-3a*$^{-/-}$ larvae at 48 hpf. Quantitation of the signal in red rectangle showed at the right panel (10 larvae for each, 3 replicates). (C) O-dianisidine staining indicated that co-injection of *hif-3a* mRNA partially restored hemoglobin levels in *hif-3a*$^{-/-}$ larvae as compared to co-injection of GFP mRNA at 36 hpf. *Hif-3a* and GFP mRNA, 750 pg/embryo. Quantitation showed at the bottom panel (6 larvae for each, 3 replicates). (D) Expression levels of the erythrocytic markers *gata1*, *alas2*, *band3*, were restored by injection of *hif-3a* mRNA in *hif-3a*$^{-/-}$ embryos as compared to the injection of the GFP mRNA control at 24 hpf. Quantitation showed at the right panel (10 larvae for each, 3replicates). (E) Expression levels of the erythrocytic markers *hbae1*, *hbae3* and *hbbe1*, were

restored by injection of *hif-3a* mRNA in *hif-3a*$^{-/-}$ embryos as compared to the injection of the GFP mRNA control at 48 hpf. Quantitation showed at the right panel (10 larvae for each, 3 replicates). The number of stained embryos was indicated in the left lower corner of each representative picture. hpf, hours post-fertilization; M1, mutant 1. Error bars indicate the standard error of the mean (S.E.M.); *$p < 0.05$; **$p < 0.01$; ***$p < 0.001$.

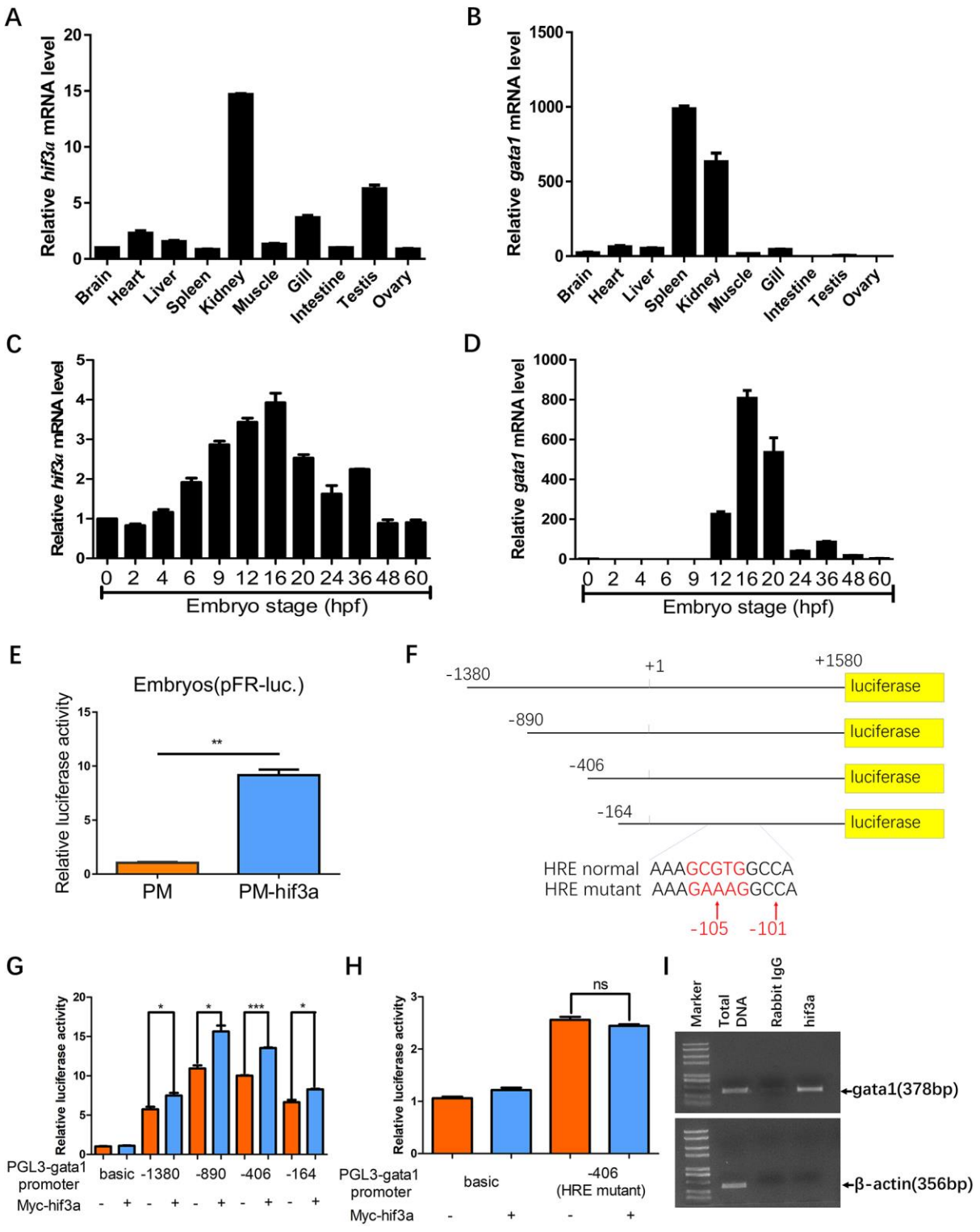

Figure 4. *Hif-3a* activates *gata1* expression by directly binding to and recognizing the hypoxia-response element (HRE) site located in the *gata1* promoter. (A) Expression pattern of *hif-3a* in zebrafish tissues (3 adults; 3 mpf). (B) Expression pattern of *gata1* in zebrafish tissues (3 adults; 3 mpf). (C) Expression pattern of *hif-3a* at different developmental stages (30 embryos). (D) Expression pattern of *gata1* at different

developmental stages (30 embryos). (E) Luciferase reporter assays indicate that *hif-3a* has transcriptional activity (50 embryos). PM/PM-hif-3a, 37.5 pg/embryo; pFR, 28.1 pg/embryo; PTK, 25 pg/embryo. (F) Schematic depiction of different deletion constructs of the *gata1* promoter luciferase reporter. (G) Luciferase reporter assays for different deletion constructs of the *gata1* promoter in the presence or absence of myc-Hif-3a in EPC cells. ("+1" is designated as the transcription initiation site; the translation starting site (ATG code) is located at "+1580"). (H) When the potential HRE site located in the *gata1* promoter was mutated, the induction of *gata1* promoter activity by *hif-3a* was lost in EPC cells. Plus signs (+) indicate the components of the expression vectors transfected. Values graphed are the means of three independent experiments performed in triplicates; error bars indicate the standard error of the mean (S.E.M.). (I) Chromatin immunoprecipitation assay (ChIP) using anti-hif-3α antibody showed that hif-3α binds to the promoter of *gata-1* directly in zebrafish embryos (about 700 embryos for each, 3 replicates; 24hpf). qRT-PCR experiments were repeated 3 times. hpf, hours post-fertilization. Error bars indicate the standard error of the mean (S.E.M.); ns, not significant; *$p < 0.05$; **$p < 0.01$; ***$p < 0.001$.

Supplementary Figure S1

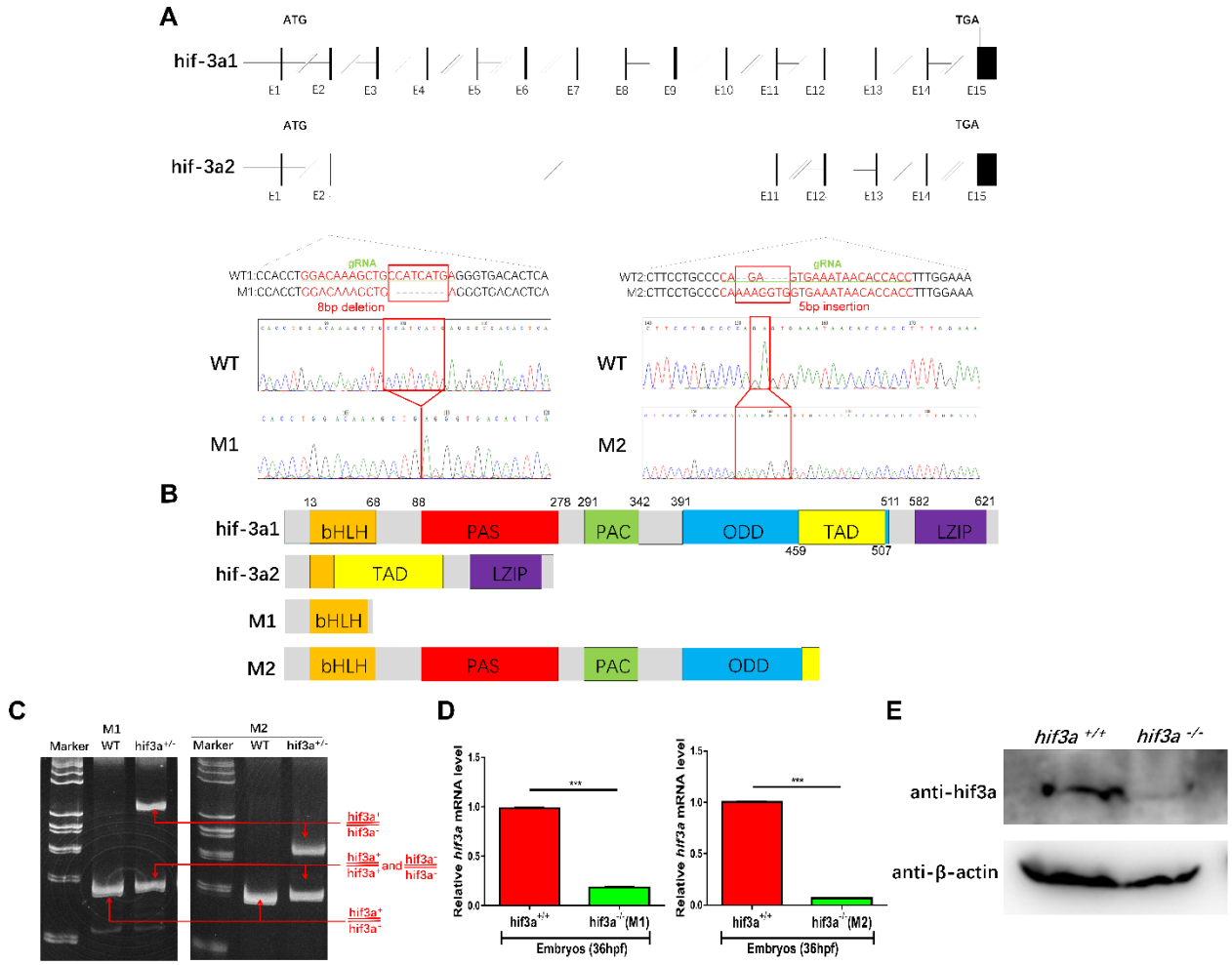

Figure S1. Generation of *hif-3a*$^{-/-}$ zebrafish using CRISPR/Cas9 technology. (A) Schematic of the targeting site in *hif-3a* and the resulting nucleotide sequence in mutant 1 (M1: *Hif-3a*$^{ihb20180620/ihb20180620}$) and mutant 2 (M2: *hif-3a*$^{ihb20180621/ihb20180621}$). (B) The predicted protein products of *hif-3a* in the mutants and their wild-type siblings. (C) Verification of the efficiency of CRISPR/Cas9-mediated disruption of zebrafish *hif-3a* disruption by heteroduplex mobility assay (HMA). (D) The relative mRNA expression levels of *hif-3a* in the wild-type zebrafish and the homozygous mutants (10 embryos for each, 3 replicates; 36 hpf) were quantified by qRT-PCR. (E) *hif-3a* protein level in the wild-type and homozygous mutant embryos (200 embryos) under normoxic conditions detected by anti-hif-3a antibody. *** $p < 0.001$.

Supplementary Figure S2

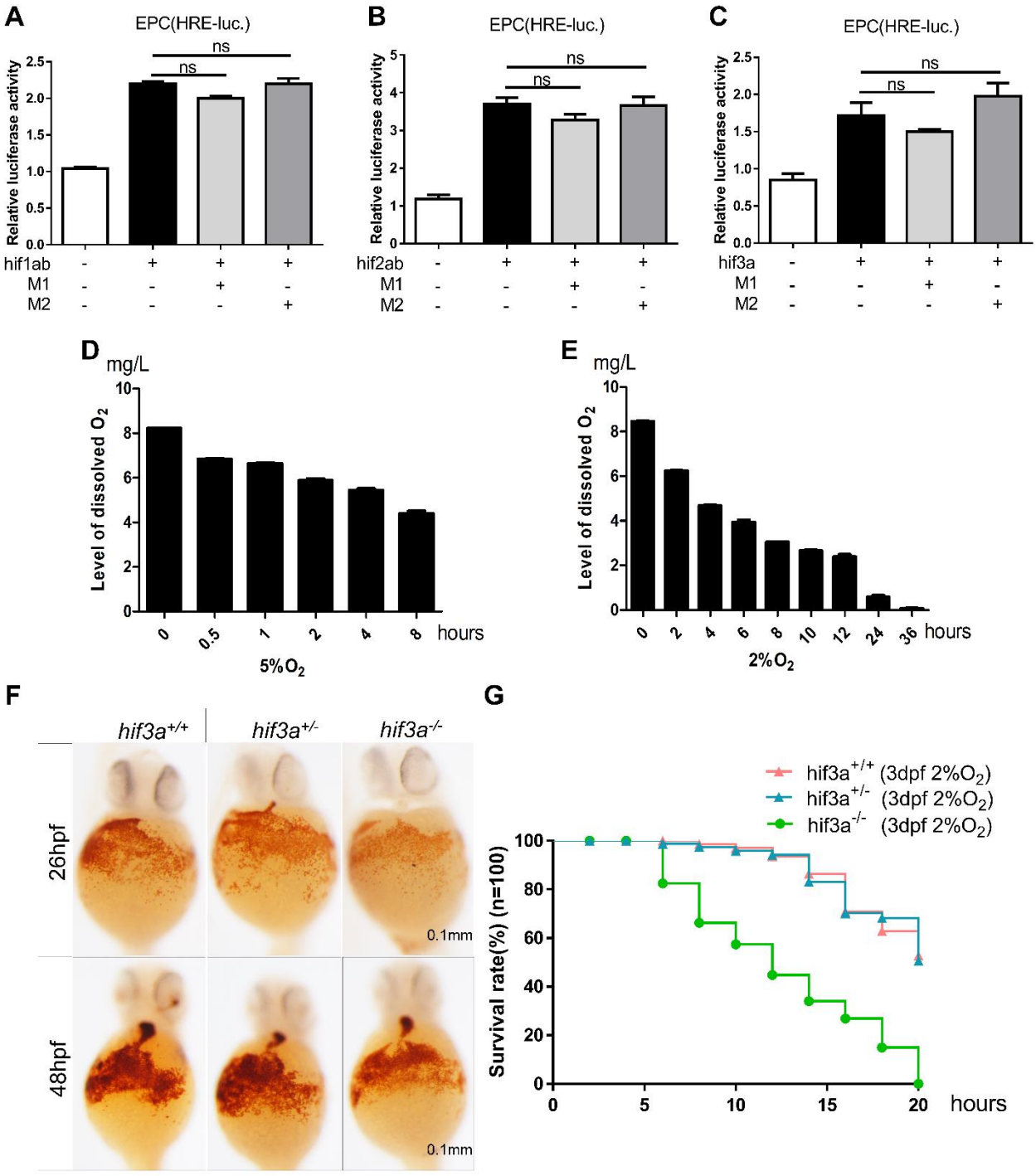

Figure S2. (A, B, C) The predicted truncated proteins in M1 and M2 mutants had no effect on the transcriptional activity of *hif-1ab, hif-2ab* and *hif-3a.* (D, E) The actual levels of dissolved O_2 in water were measured with an LDO101 probe at different time points when the flasks were put into Invivo2 Hypoxia workstation set at 5% O_2 and 2% O_2 respectively (3 replicates). (F) O-dianisidine staining of functional hemoglobin in the mature primitive erythrocytes in *hif-3a*$^{+/+}$ (left), *hif-3a*$^{+/-}$ (middle) and *hif-3a*$^{-/-}$ zebrafish (right) at 26 hpf and 48hpf. (G) The survival rate curve of *hif-3a*$^{-/-}$ zebrafish larvae, *hif-3a*$^{+/-}$ zebrafish larvae and their WT siblings (100 larvae). The oxygen concentration of the hypoxia workstation (Ruskinn INVIVO2 400) was adjusted to 2% prior to experimentation. The dead larvae were counted once every two hours. M1, mutant1; M2, mutant 2; hpf, hours post-fertilization; dpf, days post-fertilization.

Supplementary Figure S3

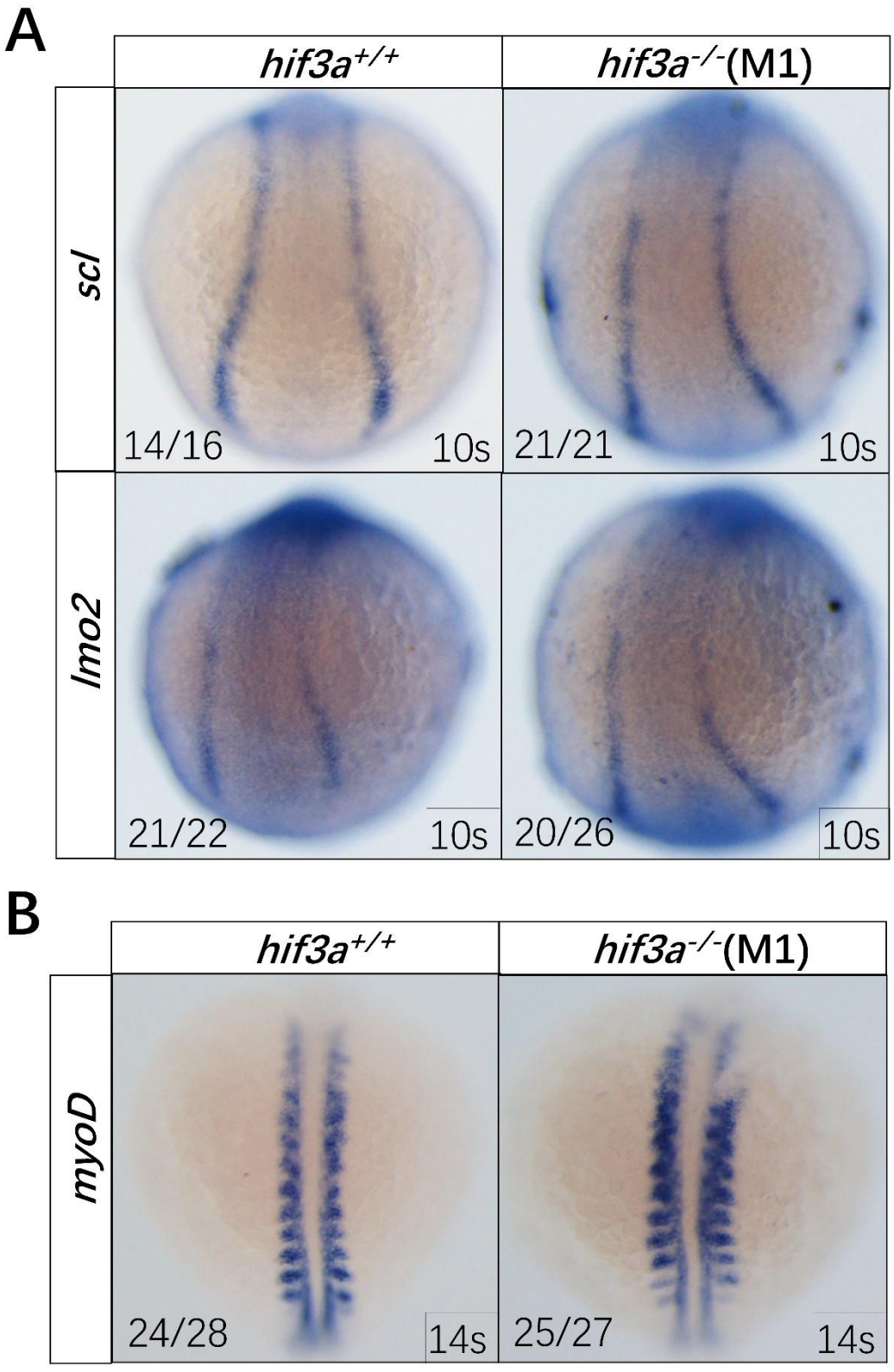

Figure S3. (A) Disruption of *hif-3a* did not alter the expression of *scl* and *lmo2* at the 10 s stage in the posterior lateral mesoderm. (B) Disruption of *hif-3a* did not alter the expression of *myoD* (the somatic mesoderm marker) at 14 s. The number of stained embryos was indicated in the left lower corner of each representative picture. M1, mutant 1; s, somite.

Supplementary Figure S4

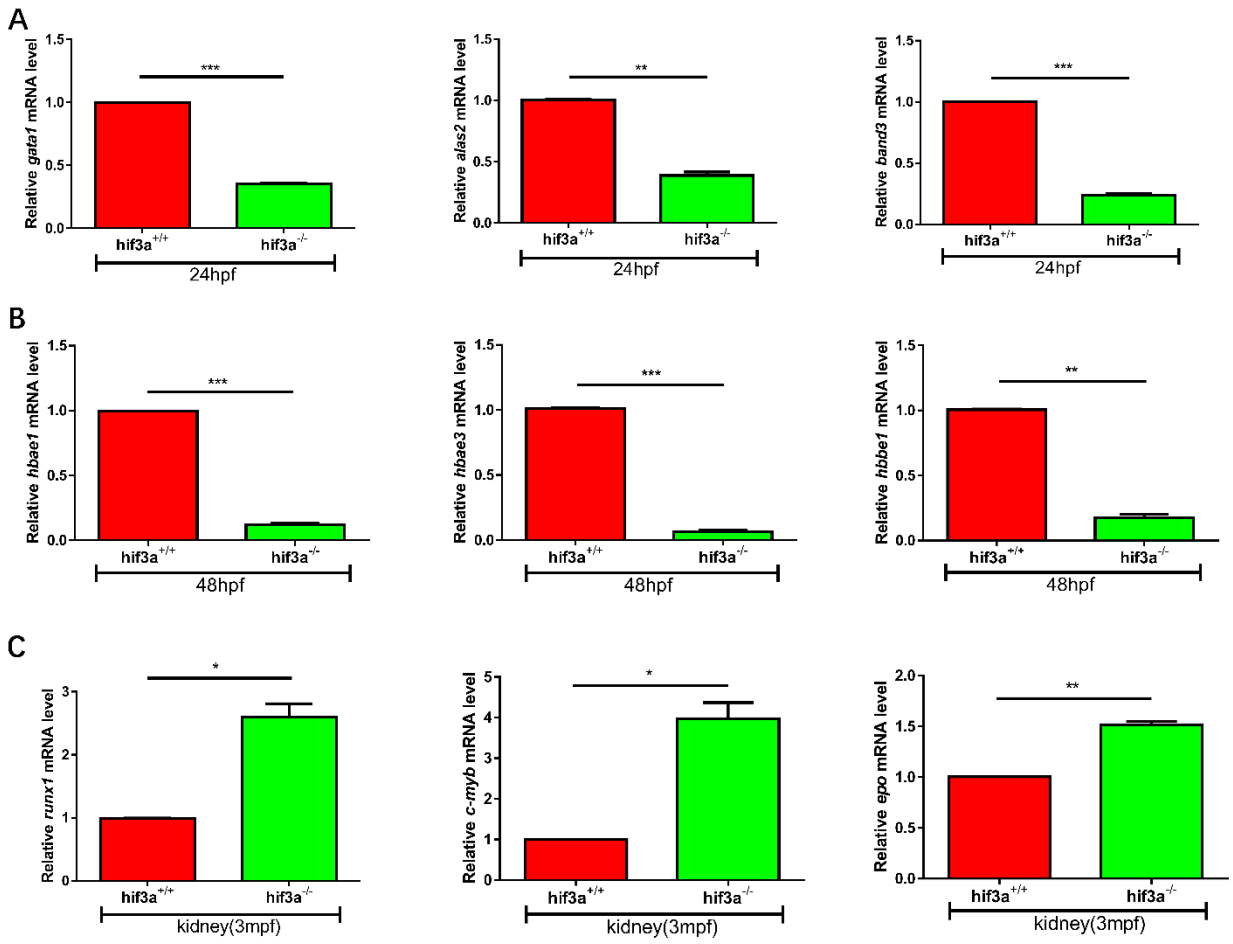

Figure S4. (A) qRT-PCR assays confirmed that the expression levels of *gata1*, *alas2*, and *band3* were reduced in *hif-3a*-null larvae at 24 hpf (30 embryos for each, 3 replicates). (B) Quantitative RT-PCR assays confirmed that the expression levels of *hbae1*, *hbae3* and *hbbe1* were reduced in *hif-3a*-null larvae at 48 hpf (30 embryos for each, 3 replicates). (C) qRT-PCR assays showing that the expression levels of *runx1, c-myb* and *epo* were increased in *hif-3a*-null kidneys at 3 mpf (3 replicates). hpf, hours post-fertilization; mpf, months post-fertilization. * $p < 0.05$; ** $p < 0.01$; *** $p < 0.001$.

Supplementary Figure S5

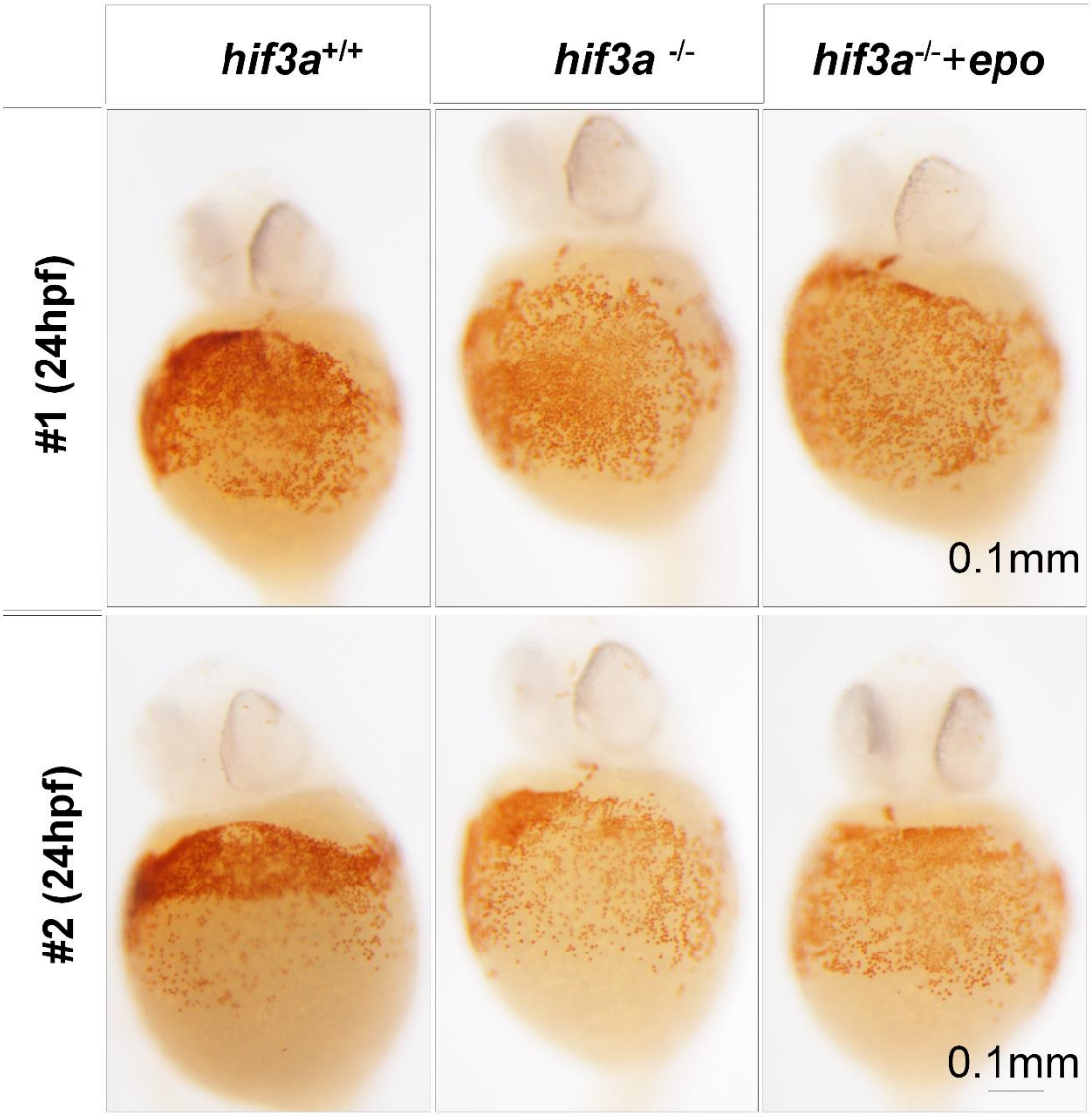

Figure S5. O-dianisidine staining indicated that co-injection of *epo* mRNA (500 pg/embryo) could not restore hemoglobin levels in *hif-3a*$^{-/-}$ larvae at 24 hpf. hpf, hours post-fertilization.

Supplementary Figure S6

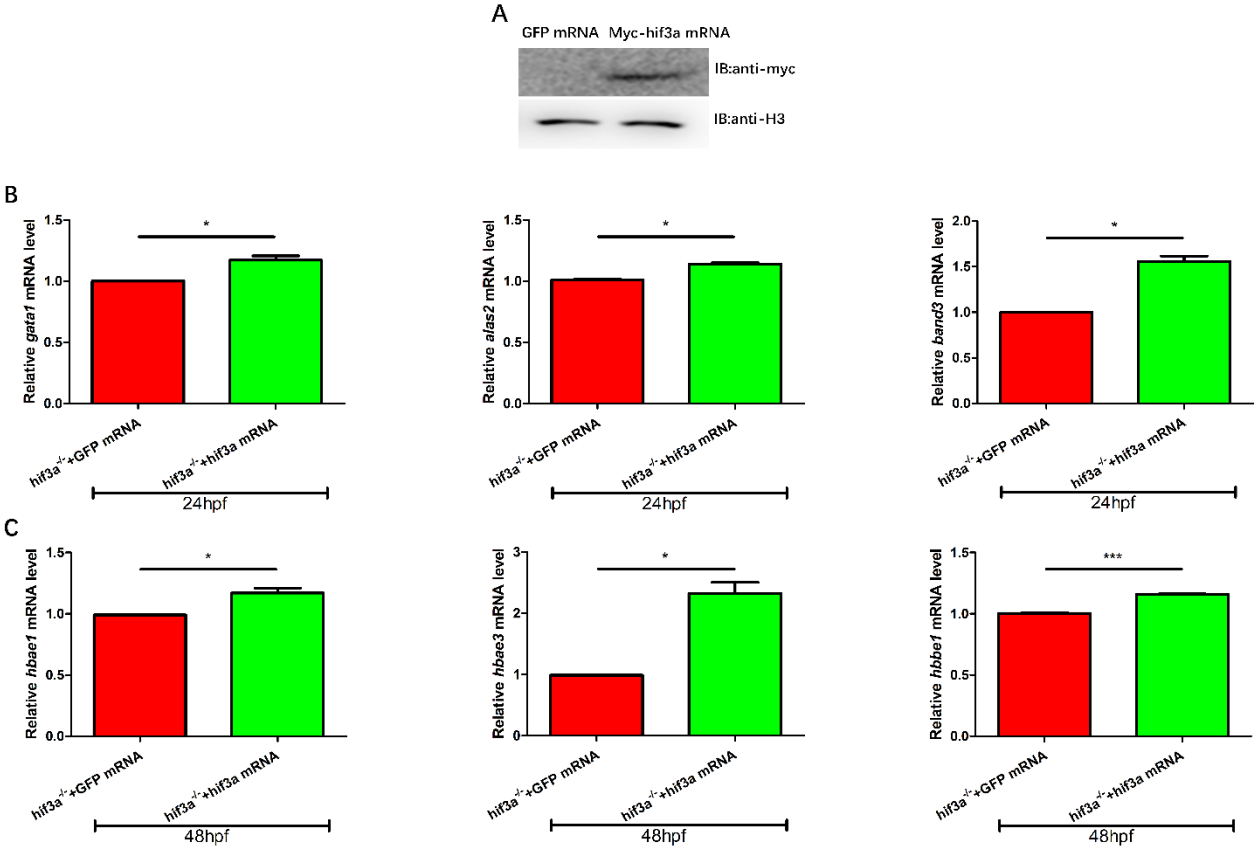

Figure S6. (A) Expression of myc-hif-3a in the injected embryos was confirmed by western blot assays (200 embryos). (B) qRT-PCR confirmed the restoration of *gata1*, *alas2* and *band3* by injection of *hif-3a* mRNA in *hif-3a*-null embryos at 24 hpf as compared with by the injection of the GFP mRNA control. (C) qRT-PCR confirmed the restoration of *hbae1*, *hbea3* and *hbbe1* by the injection of *hif-3a* mRNA in *hif-3a*-null embryos at 48 hpf as compared to the injection of the GFP mRNA control. IB, immunoblotting; hpf, hours post-fertilization. 30 embryos for each, 3 replicates; * $p < 0.05$;*** $p < 0.001$.

Supplementary Figure S7

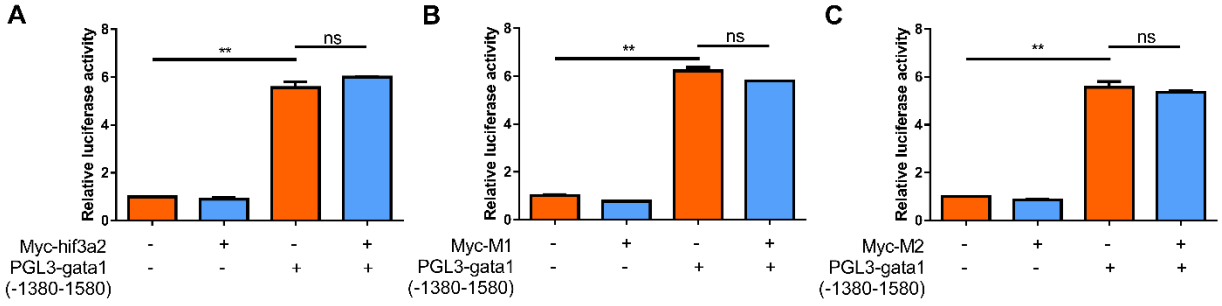

Figure S7. Luciferase reporter assays indicate that *hif-3a2*(A), *hif-3a* mutant M1(B) and M2(C) could not active *gata1* promoter in EPC cells. ** $p < 0.01$; ns, no significance.

Supplementary Figure S8

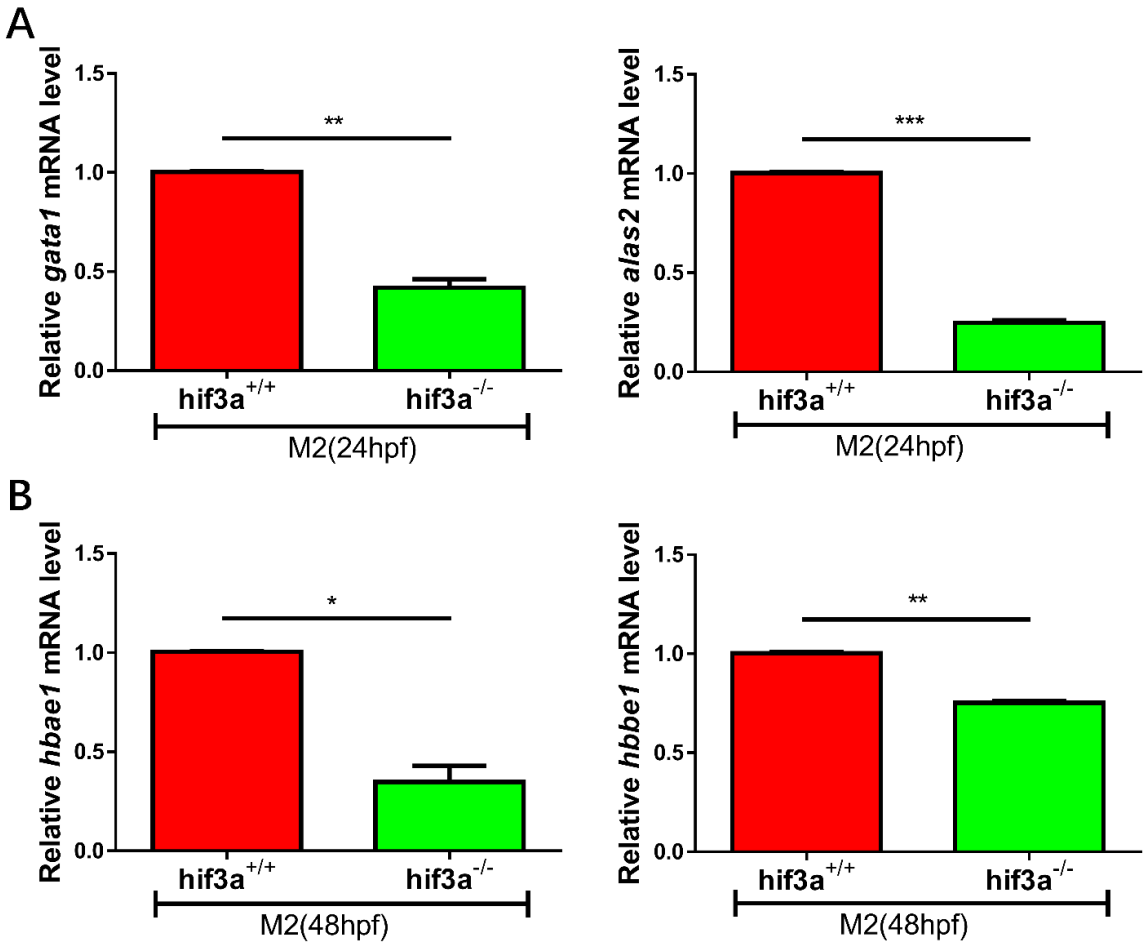

Figure S8. (A) Expression levels of erythrocytic markers *gata1* and *alas2* in wild-type and *hif3a*$^{-/-}$ (M2: *hif1al*$^{ihb20180621/ihb20180621}$) zebrafish larvae at 24 hpf. (B) Expression levels of *hbae1* and *hbbe1* were quantified by qRT-PCR at 48hpf. Values graphed are the means of three independent experiments performed in triplicates; error bars indicate the standard error of the mean (S.E.M.). hpf, hours post-fertilization. n=30; * $p < 0.05$; ** $p < 0.01$; *** $p < 0.001$.

Supplementary Figure S9

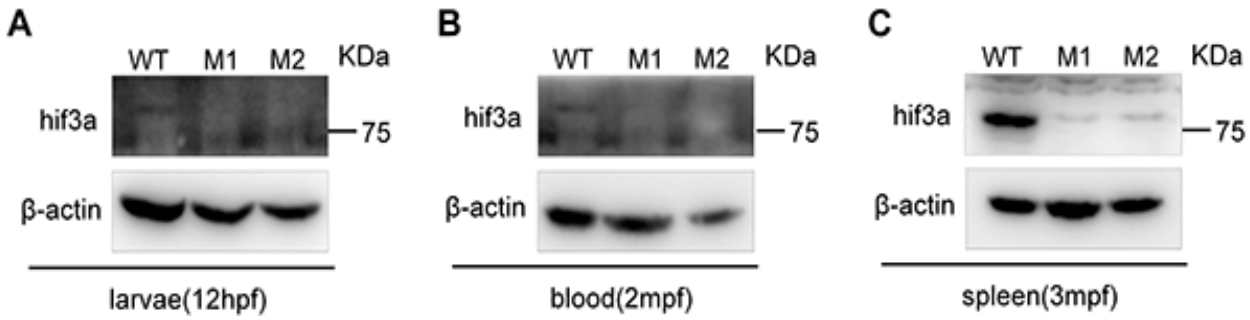

Figure S9. (A, B, C) Western blot analysis of hif-3a protein level in larvae (12hpf; 200 embryos), blood (2mpf; 3 zebrafish for each, 3 replicates) and spleens (3mpf; 3 zebrafish for each; 3 replicates) from wild-type and M1, M2 mutants. WT, wildtype; M1, mutant 1; M2, mutant 2; mpf, months post-fertilization.

Supplementary Figure S10

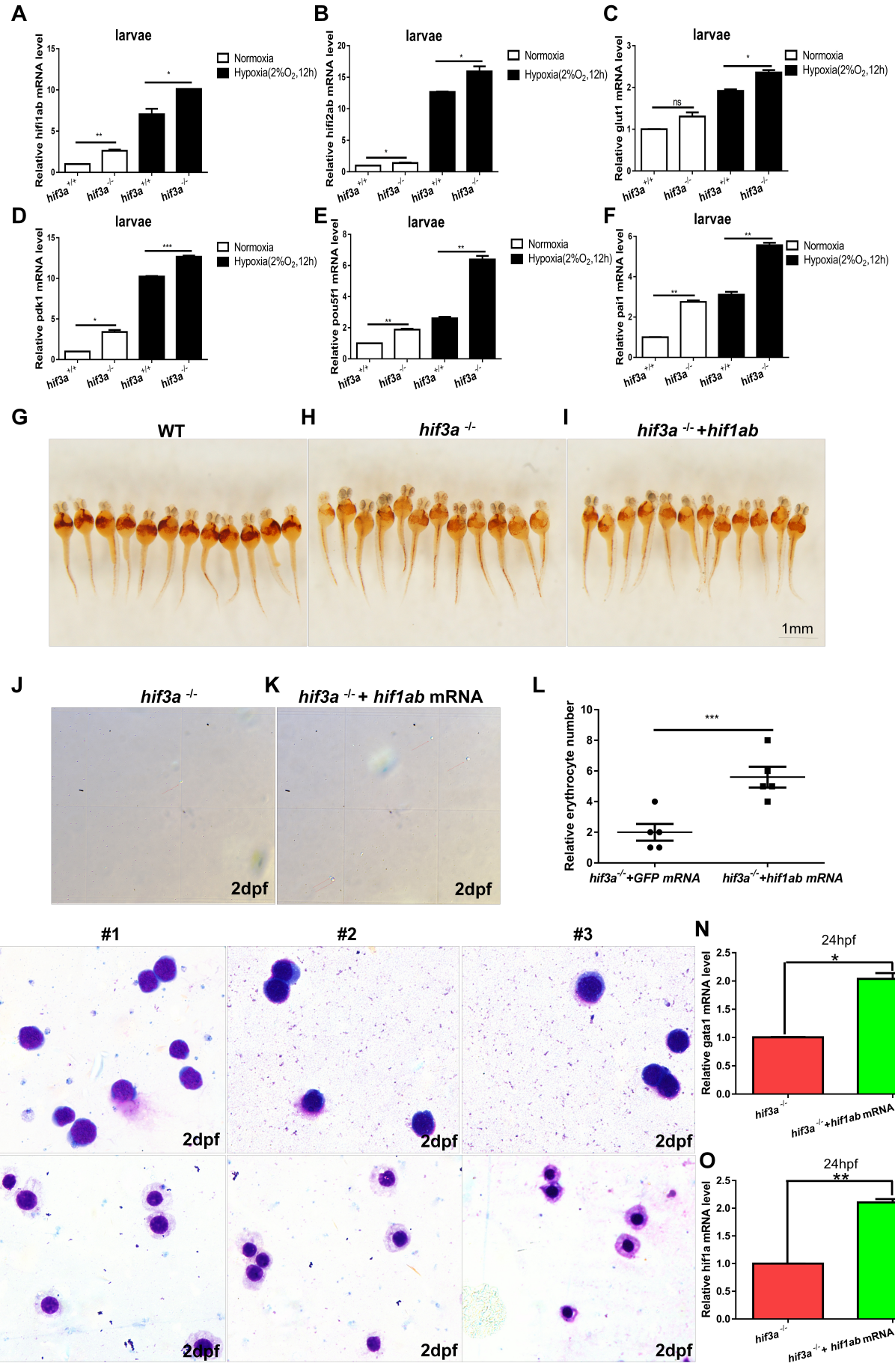

Figure S10. (A, B) qRT-PCR analysis of *hif1a*(A) and *hif2a*(B) expression in WT(*hif-3a*$^{+/+}$) and *hif- 3a*-null(*hif-3a*$^{-/-}$) zebrafish embryo (10 embryos for each, 3 replicates; 3dpf) under normoxia and hypoxia (2% O_2 for 12 hours). (C-F) Expression levels of the *hif-1a* down-stream targets *glut1*(C), *pdk1*(D) and *hif-2a* down-stream targets *pou5f1*(E), *pai1*(F) were increased in *hif-3a*$^{-/-}$ larvae (10 embryos for each, 3 replicates; 3 dpf) under normoxia and hypoxia (2% O_2 for 12 hours). (G-I) O-dianisidine staining indicated that co-injection of *hif-1ab* mRNA (500 pg/embryo) partially restored hemoglobin levels in *hif-3a*$^{-/-}$ larvae at 2 dpf. (J-K) Erythrocyte number counting indicated that co-injection of *hif-1ab* mRNA (500 pg/embryo) increased erythrocyte in *hif-3a*$^{-/-}$ larvae at 2 dpf. (M) May-Grunwald-Giemsa staining indicated that co-injection of *hif-1ab* mRNA (500 pg/embryo) restored erythrocytic maturation in *hif-3a*$^{-/-}$ larvae at 2 dpf. (N) Co-injection of *hif-1ab* mRNA (500 pg/embryo) restored gata1 expression in *hif-3a*$^{-/-}$ embryos at 24 hpf. (O) Expression of micro-injected *hif-1ab* mRNA in *hif-3a* $^{-/-}$ embryos at 24 hpf was confirmed by qRT-PCR. Hpf, hours post fertilization; dpf, days post-fertilization. *$p < 0.05$; ** $p < 0.01$; ***$p < 0.001$.

Supplementary Figure S11

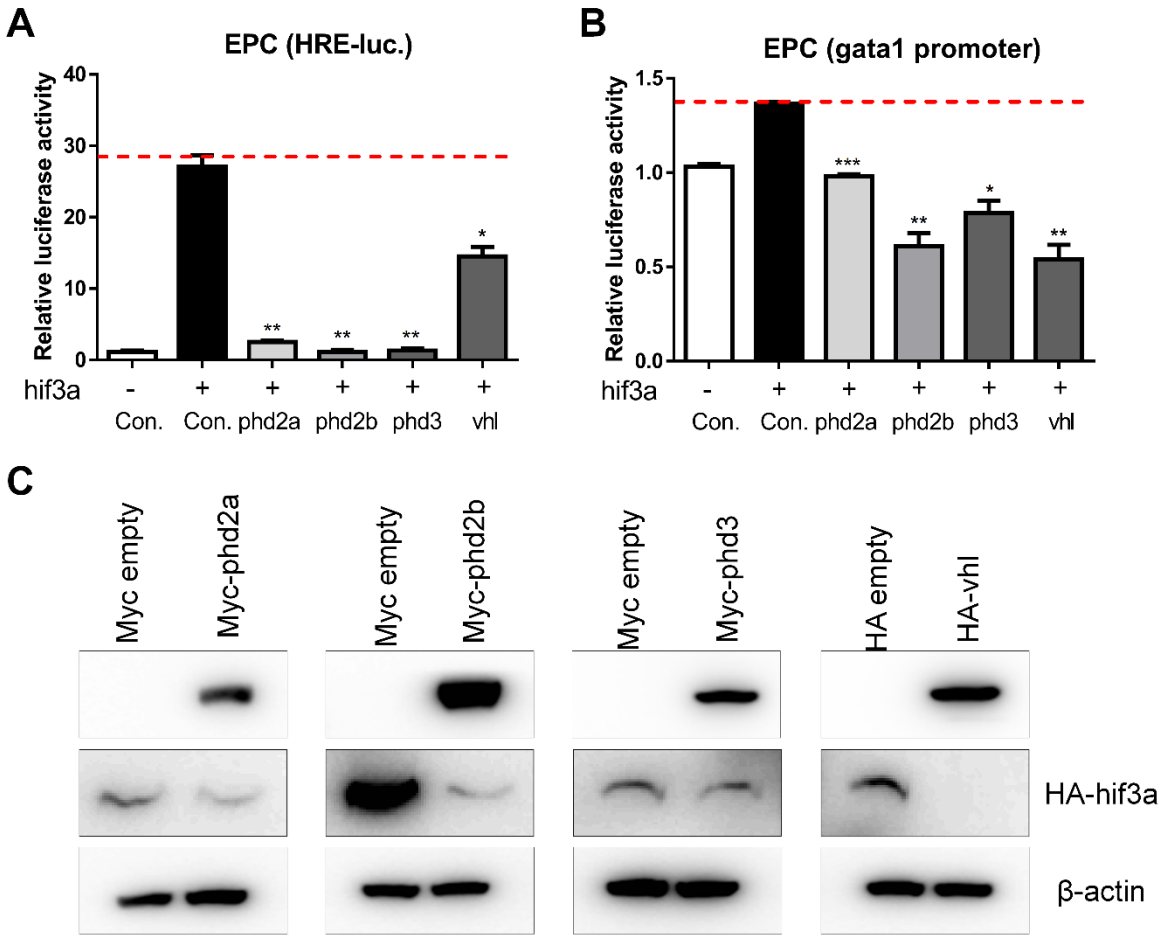

Figure S11. (A) Co-expression of *phd2a, phd2b, phd3* and *vhl* together with *hif-3a* suppressed the activity of HRE luciferase reporter induced by hif-3a in EPC cells. (B) Co-expression of *phd2a, phd2b, phd3* and *vhl* together with *hif-3a* suppressed the activity of gata1 promoter luciferase reporter induced by hif-3a in EPC cells. *$p < 0.05$; ** $p < 0.01$; ***$p < 0.001$. (C) Western blot analysis indicated that hif-3a protein level was decreased when *phd2a, phd2b, phd3* or *vhl* were co-expressed in EPC cells. Con, control. Myc empty, pCMV-Myc empty vector.

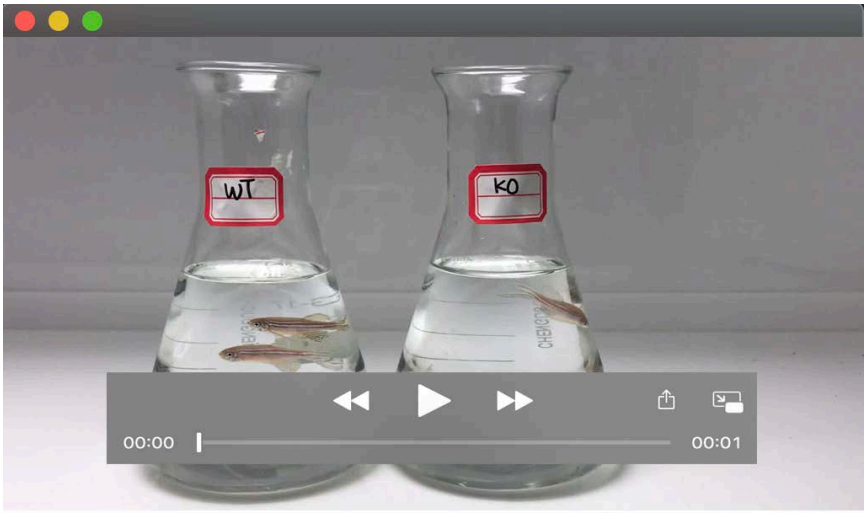

Movie 1. Wildtype (left, WT) and *hif3-a* null (right, KO) zebrafish (3 mpf, body weight = 0.32 ± 0.02 g) placed in a hypoxia workstation at the beginning (5% O_2) (before 30 min).

Movie 2. Wildtype (left, WT) and *hif3-a* null (right, KO) zebrafish (3 mpf, body weight = 0.32 ± 0.02 g) placed in a hypoxia workstation for a while (5% O_2).